AD-766 158

STUDIES OF E-BEAM PUMPED MOLECULAR LASERS

Donald J. Eckstrom, et al

Stanford Research Institute

Prepared for:

Office of Naval Research
Advanced Research Projects Agency

31 July 1973

Semiannual Technical Report No. 2
Covering the Period January 1 to June 30, 1973

July 31, 1973

STUDIES OF E-BEAM PUMPED MOLECULAR LASERS

By D. J. ECKSTROM, R A GUTCHECK R M. HILL,
D. HUESTIS, and D C LORENTS

SRI #MP 73-1

Prepared for:

ADVANCED RESEARCH PROJECTS AGENCY
WASHINGTON, D.C. 20301

DIRECTOR, PHYSICS PROGRAMS, PHYSICAL SCIENCES DIVISION
OFFICE OF NAVAL RESEARCH
DEPARTMENT OF THE NAVY
800 NORTH QUINCY STREET
ARLINGTON, VIRGINIA 22217

Sponsored by:

ADVANCED RESEARCH PROJECTS AGENCY
ARPA Order No. 1807 Program Code No. 3E90
CONTRACT N00014-72-C-0478 (15 April 1972 - 31 December 1973)
Contract Amount $159,885 SRI Project PYU-1925

STANFORD RESEARCH INSTITUTE
Menlo Park, California 94025 · U.S.A.

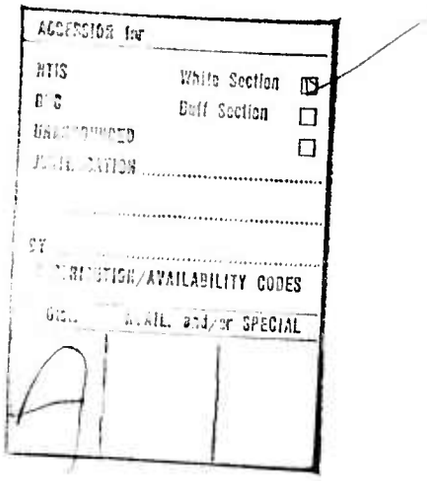

The views and conclusions contained in this document are those of the authors and should not be interpreted as necessarily representing the official policies, either expressed or implied, of the Advanced Research Projects Agency of the U.S. Government.

Security Classification

DOCUMENT CONTROL DATA - R & D

Security classification of title, body of abstract and indexing annotation must be entered when the overall report is classified)

1. ORIGINATING ACTIVITY (Corporate author)
Stanford Research Institute
333 Ravenswood Avenue
Menlo Park, California 94025

2a. REPORT SECURITY CLASSIFICATION
Unclassified

2b. GROUP

3. REPORT TITLE
STUDIES OF E-BEAM PUMPED MOLECULAR LASERS

4. DESCRIPTIVE NOTES (Type of report and inclusive dates)
Semiannual Technical Report No. 2 Where is No. 1?

5. AUTHOR(S) (First name, middle initial, last name)
Donald J. Eckstrom, Robert M. Hill, Robert A. Gutcheck, David L. Huestis, and Donald C. Lorents

6. REPORT DATE
July 31, 1973

7a. TOTAL NO. OF PAGES

7b. NO. OF REFS

8a. CONTRACT OR GRANT NO
N00014-72-C-0478

b. PROJECT NO
PYU 1925

c.

d.

9a. ORIGINATOR'S REPORT NUMBER(S)
SRI MP73-1

9b. OTHER REPORT NO(S) (Any other numbers that may be assigned this report)

10. DISTRIBUTION STATEMENT
Distribution of this document is unlimited.

11. SUPPLEMENTARY NOTES

12. SPONSORING MILITARY ACTIVITY
Advanced Research Projects Agency
Order No. 1807, Program Code No. 2C90

13. ABSTRACT

This report covers experimental and theoretical work on the feasibility of attaining laser action in high pressure gases excited by electron beam pulses. The radiative decay of Hg_2 dimers has been measured as well as the existence of net absorption of excited Hg_2. It is concluded that direct laser action by Hg_2 is unlikely. A reappraisal of the Hg_2 states is presented. Initial experimental studies of Ar + N_2 mixtures are presented that show general agreement with model calculations and the ability to create large useable populations of metastable excited N_2.

DD FORM 1 NOV 68 1473 (PAGE 1)
S/N 0101-807-6801

Security Classification

14 KEY WORDS	LINK A		LINK B		LINK C	
	ROLE	WT	ROLE	WT	ROLE	WT
Hg dissociation laser						
Energy transfer						
E-beam pumping						
Rare gas dimers						

CONTENTS

FIGURES

TABLES

SUMMARY

The purpose of this program is to develop an understanding of the molecular kinetics pertinent to new high efficiency, high power lasers. We are studying high pressure gases that are initially pumped by intense bursts of electrons (10^3 amperes, 500 keV, 3×10^{-9} sec), since these systems could have efficiencies of more than 10% and also short pulse, high power capability. This energy, which is primarily deposited by creating atomic ions, rapidly collects in the lowest molecular excited state. Laser radiation from this state is possible either when the ground state is repulsive, that is, when no bound, ground molecular state exists (e.g., the rare gases and Hg, Cd, and Zn), or when the upper laser state radiates primarily to higher vibrational levels of the ground state. In this report we describe studies of a gas with a repulsive ground state, the mercury dimer Hg_2, and of a gas mixture that will satisfy the second criterion, $Ar + N_2 + NO$.

The Hg_2 dimer is formed by the association of a ground state Hg atom with an electronically excited, metastable Hg atom. At high pressure the dimer radiates a continuum centered near 4500 A extending 500 A to either side. We have shown that the radiative decay time for this dimer is quite slow ($\sim 1.4 \times 10^{-5}$ sec) and that the self quenching of the excited dimer state is not very rapid. These characteristics make Hg_2 a very attractive candidate for an efficient laser medium. Unfortunately, we also find that the absorption cross section of the dimer is greater than the stimulated emission cross section, resulting in net absorption throughout the continuum band. We have concluded that laser action in mercury is unlikely.

Mercury remains an attractive medium for energy storage, but practical use of this storage would be greatly helped by a better

understanding of the molecular states of Hg_2. We include in this report a reappraisal of these states intended to stimulate further thinking on this long-standing problem.

Rare gas dimers, in particular Xe_2 and Kr_2, have already demonstrated laser action but with disappointing efficiencies. This problem, coupled with the relatively high gain implying low energy storage capacity and with vacuum ultraviolet wavelengths, has led us to consider ways of transferring the energy deposited in the rare gas to other gas molecules in order to improve total efficiency, shift the wavelength to the ultraviolet or visible, and improve the energy storage capacity.

Our initial results on the mixture Ar + N_2 are given in this report. This combination was chosen because most of the reactions of interest have been quantitatively studied and because the nitrogen triplet system of excited states offers good candidates for lasing in the near ultraviolet as well as a very long-lived metastable state with excellent energy storage potential.

We have observed radiation from the nitrogen C and B excited triplet states and used small additions of NO gas as a monitor of the metastable $N_2(A)$ state population. The energy in $N_2(A)$ can transfer almost resonantly to excite NO(A) which then radiates rapidly.

Our preliminary conclusions are essentially favorable:

(1) Energy can be rapidly transferred from the dimer Ar_2 produced by the electron beam excitation to the nitrogen triplet states.

(2) A model based on the known reaction rates predicts the overall time history of the observed excitation and radiation. A derived number density of metastable $N_2(A)$ agrees reasonably well with the model prediction. Detailed

comparison of model and experiment appears to be practical.

(3) Large populations of metastable $N_2(A)$ can be produced. The maximum population is critically dependent on the rate of self-destruction, i.e., $N_2(A)$ colliding with $N_2(A)$. This rate constant can be measured in our experiment and will determine the practicality of using N_2 for high energy storage.

The initial agreement of model and experiment leads us to think that Ar + N_2 + NO might be a reasonably efficient lasing medium in the ultraviolet. The electron beam energy is deposited in the argon and transferred to the N_2 system before it can be radiated away. The energy is tnen transferred from the $N_2(A)$ state to the NO(A) state in a time comparable to the NO radiative lifetime. Lasing should occur between the ground vibrational state of NO(A) and the second or third vibrational level of the NO ground state. This possibility will be tested in the next period.

I. INTRODUCTION

An overview of the motivation and progress in this program is given in the preceding summary. More detailed discussions of techniques, results, and conclusions can be found in the following sections. The work on mercury dimers Hg_2 is discussed in Section II and in the appendices, which are preprints of papers accepted for publication. Our experiments, analysis, and modeling on mixtures of Ar, N_2, and NO excited by a Febetron are given in Section III. Section IV is a compilation of our conclusions.

II MOLECULAR MERCURY STUDIES

Summary of Experimental Work

The primary objective of the research during the first year of this contract and continuing into this second year has been to determine the feasibility of laser action in the blue-green continuum band of the mercury excimer. This possibility was first pointed out by Houtermann[1] in 1960 and was attempted in 1968.[2] The development of high energy, high current, short pulse electron beam machines has a again raised the hope of such achievement.

The experimental setup and some of the observations and results from our study of Hg were presented in the first semiannual report.[3] Briefly, we measured both atomic and molecular radiation from mercury vapor following excitation by the 3-nsec, 10-joule electron pulse from a Febetron 706. Vapor pressures ranged from 0.2 to 10 atmospheres. The most pertinent results of that phase of the study were the determination of a radiative lifetime of 14 ± 3 μsec for both the 3350 and the 4850 Å continuum bands of Hg_2^* and the discovery of an important bimolecular collisional deactivation of the Hg_2^* excimer:

$$Hg_2^* + Hg_2^* \rightarrow Hg_2^{**} + 2Hg$$

with a rate on the order of 10^{-11} cm^3/sec. These results have been described in some detail in a short paper that will be published in Chemical Physics Letters. The preprint is included as Appendix A of this report.

While the relatively long radiative lifetime and the bi-excimer collisional deactivation make it difficult to achieve the excimer populations required for high gain, they do not preclude the achievement of laser action. Therefore, we carried out a series of measurements of the

optical gain of the excited Hg vapor as a function of time and of wavelength in the 4800 Å band. Time resolved measurements were made using a cw Ar^+ laser at seven wavelengths between 4579 and 4145 Å. The variation of gain with wavelength over the range from 3900 to 4900 Å at a single time following the excitation pulse was measured using the continuum radiation from a 10-nsec, 10^3-watt flashlamp (Optitron Model NR-1). These experiments and their results are described in a second paper, attached as Appendix B, which will be published in Applied Physics Letters. It was found that the gain was negative at all wavelengths tested, with virtually no structure to the absorption except near atomic lines. Furthermore, the absorbing state was identified as the upper level of the transition producing the 4850 Å band. We conclude that the upper level of the absorptive transition is a repulsive electronic state of Hg_2; therefore gain (and therefore laser action) is unlikely anywhere in the band.

Since we have concluded that direct laser action on the visible mercury continuum is very unlikely we have stopped work on the system, which included analysis of the spectroscopic data and computer modeling of the reaction kinetics. Because of its relatively long radiative lifetime, however, Hg_2^* is still an attractive candidate for energy storage, with subsequent transfer to another radiating species. In particular, the Hg + Br_2 system may be of interest, since HgBr which would be formed in the excitation pulse, has a band system at 4900 ± 100 A.

Complementing our work on mercury, Professor Green and his coworkers at the University of Florida, Gainesville, have completed their subcontract work on electron impact cross sections for mercury. Their final report entitled, "Electron Impact Cross Sections for the Element Mercury," by J. N. Bass, R. A. Berg, and A.E.S. Green, has been modified only slightly from their

preliminary report which was published as Appendix B of our first semi-annual report.[3] Copies of this final report may be obtained from Professor Green at Gainesville. The report will also be submitted for publication in the open literature in the near future.

It should be noted in concluding the discussions of our mercury experiments that, in spite of extensive studies over more than 40 years, no explanation of the molecular mercury state structure has yet been advanced that satisfactorily explains all the observed properties of the molecular radiation. In particular, the continuum bands of Hg_2 centered at 3350 and 4800 Å have generally been identified with transitions from the $Hg_2^* \; {}^3 1_u$ and ${}^3 0_u^-$ states to the repulsive ${}^1\Sigma_g^+$ ground state. This requires an energy separation of the two upper states of ~9000 cm^{-1}. This energy separation would be due to spin-orbit coupling, but our calculations (described below) indicate that the separation should be no more than ~200 cm^{-1}. There is also considerable difficulty in explaining the observed common lifetime of the two continuum bands. If the bands originate from states with substantially different energies, then a pressure-dependent decay of the higher energy level would be expected because of collisional relaxation effects.

In the next subsection, we describe a new analysis of Hg_2 that leads to a state structure different from that currently assumed. This new model contradicts some spectroscopic assignments of the current model and offers some alternative assignments that qualitatively explain many of the observations. While some difficulties remain, this new model seems to be an important first step in resolving an old and intriguing problem.

The State Structure of Hg_2

In view of the continuing confusion over the interpretation and assignment of the multitude of Hg_2 absorptions and emissions, a

qualitative understanding of the expected potential curves is of particular importance. In the absence of calculated curves or detailed scattering information, we will try here to supply such a qualitative discussion of the potential curves, in the spirit of Mullikan's elucidation of the levels of Xe_2.[4-7]

The ground state of the mercury atom has the configuration $[Xe]4f^{14}5d^{10}6s^2$. The low-lying excited states correspond to excitation of one of the 6s electrons, giving a configuration of say $[Xe]4f^{14}5d^{10}6s6p$ for the 6^3P and 6^1P states. For the purpose of describing the electronic structure of the excited states of Hg_2, we can expect that core electrons, $[Xe]4f^{14}5d^{10}$ will remain relatively unchanged, or at least any changes will be common to all the lower states. Our attention will therefore be focused on the outer four electrons in Hg_2.

Only one state of Hg_2 arises from ground state atoms, $Hg(6s^2, {}^1S_o)$. The potential for this $^1\Sigma_g^+$ state is known to have only a van der Waals well about 0.12 eV deep, with a repulsive wall at smaller internuclear separation, R. This can be understood, as can the corresponding situation in He_2, by reference to the orbital correlation diagram, Figure 1. The 6s atomic orbital splits into two molecular molecular orbitals:

$$\sigma_g = \sqrt{\tfrac{1}{2}}\,(6s_\ell + 6s_r)$$

$$\sigma_u = \sqrt{\tfrac{1}{2}}\,(6s_\ell - 6s_r)$$

where $6s_\ell$ and $6s_r$ are the atomic 6s orbitals on the left and right Hg atoms, respectively. As suggested by the correlation diagram, we would call the σ_g a bonding orbital and the σ_u antibonding.

Since the ground state of Hg_2 begins at large R with four 6s electrons, the resulting σ_g and σ_u molecular orbitals are both doubly occupied. The antibonding character of the σu electrons

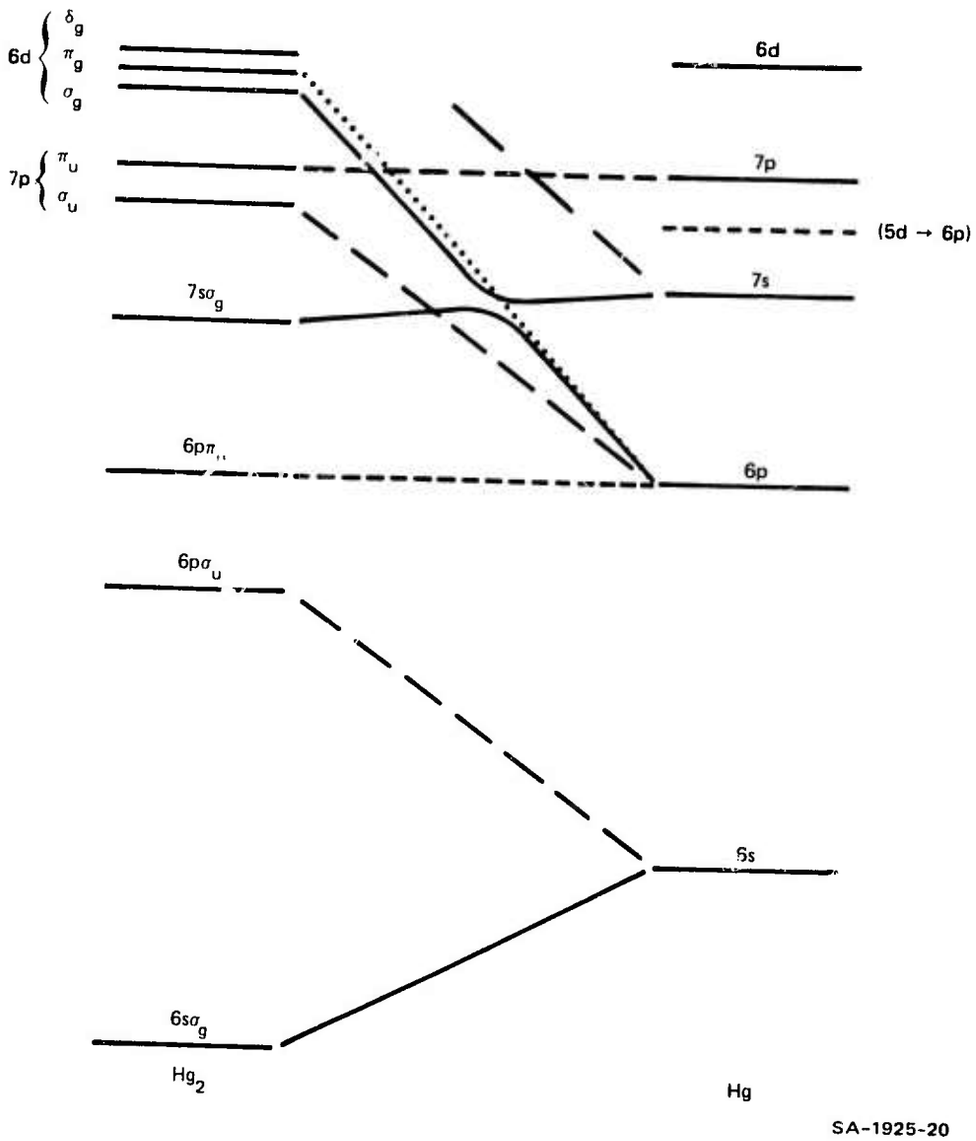

FIGURE 1 Hg_2 ORBITAL CORRELATION DIAGRAM

just about cancels the bonding of the σ_g electrons, leading to only a van der Waals well. Strong repulsion begins at smaller R as the inner 5d electrons begin to overlap.

The excited states of Hg_2 might be described by removing one of the 6s electrons and placing it in a higher orbital. This suggests that we next look at the bonding in the lowest states of Hg_2^+ that arise from this removal of one 6s electron. These two states may be represented by the configurations

$$^2\Sigma_u^+ \rightarrow (6s\sigma_g)^2(6p\sigma_u)$$

and

$$^2\Sigma_g^+ \rightarrow (6s\sigma_g)(6p\sigma_u)^2.$$

The $^2\Sigma_u^+$ state, with two bonding orbitals and only one antibonding orbital, should have a considerable binding energy (0.5 to 1.5eV). On the other hand, the $^2\Sigma_g^+$ has a net antibonding character, leading to a purely repulsive potential curve. One might like to compare with the similar situation in He_2^+ (refs. 5, 7, 8).

To describe the excited states of Hg_2^* we add to either of the Hg_2^+ configurations ($^2\Sigma_u^+$, $^2\Sigma_g^+$) one additional electron chosen from the higher orbitals in the correlation diagram. Specifically we are interested in the states that would dissociate to the 6s6p atomic configuration; therefore, the lowest $^{1,3}\Pi_{g,u}$ and $^{1,3}\Sigma_{g,u}$ states are the states of interest.

We begin with the Π_g states. The possible configurations are $(6s\sigma_g)^2(6p\sigma_u)(6p\pi_u)$ and $(6s\sigma_g)(6p\sigma_u)^2(6d\pi_g)$. The first of these will obviously be much lower in energy, as can be seen from the correlation diagram. The $6p\pi_u$ electron has almost no effect on the potential curve. The molecular $6p\pi$ orbital should be about the same size and shape as it was in the atom. There are no other electrons in the molecule with which it has much overlap. This

contrasts sharply with the situation for σ orbitals, as we will see below. In conclusion we can see that a potential curve just about paralled to $Hg_2^+(^2\Sigma_u^+)$ is expected for the Π_g states. A corresponding description also applies to the $^{1,3}\Pi_u$ states of H_2 (see reference 9 for potential curves).

To characterize the Σ_g^+ states, we could use the configurations

$$^{1,3}\Sigma_g^+ \rightarrow \begin{cases} (6s\sigma_g)^2(6p\sigma_u)(7p\sigma_u) \\ (6s\sigma_g)(6p\sigma_u)^2(6d\sigma_g) \\ (6s\sigma_g)(6p\sigma_u)^2(7s\sigma_g). \end{cases}$$

None of these can be expected to have much binding, although the first should be the least repulsive. Probably the Σ_g^+ states will have large humps, as the 6p orbital is promoted to 7p, and may have shallow minima from the core binding of $Hg_2^+(^2\Sigma_u^+)$. They will not be bound relative to the separated atoms. It appears that a nearly identical description applies to the $^1\Sigma_g^+$ state of He_2 arising from He(1s2p), in which the 2p orbital is promoted to 3p, with a large barrier and eventual minimum above the separated atom limit.[10] The height of the barrier in the Hg_2 $^{1,3}\Sigma_g^+$ states should be even larger than that in He_2 since the 6p-7p separation is almost 4 eV in Hg and the 2p-3p separation is only about 2 eV in He.

The placement of the Σ_g^+ and Π_u states is especially important, as they have been thought to be responsible for most of the optical measurements to date. The $^{1,3}\Sigma_u^+$ states should be represented by the configurations

$$\Sigma_u^+ \rightarrow \begin{cases} (6s\sigma_g)^2(6p\sigma_u)(6d\sigma_g) \\ (6s\sigma_g)^2(6p\sigma_u)(7s\sigma_g) \\ (6s\sigma_g)(6p\sigma_u)^2(7p\sigma_u) \end{cases}$$

The correlation diagram suggests that the first of these configurations is dominant at larger R. The potential curve rises as R decreases. A minimum at smaller R is expected as the $6d\sigma$ orbital crosses over to the $7s\sigma$ and the $Hg_2^+(^2\Sigma_u^+)$ binding becomes important. To repeat, the important observations are that a significant hump is to be expected and that due to orbital promotion the $^{1,3}\Sigma_u^+$ states will lie <u>above</u> the corresponding $^{1,3}\Pi_g$ states. Once again the analogy is very close with the Π_g and Σ_u states of He_2 arising from He(1s2p) (refs. 8, 10).

We expect the Π_u states to arise from the configurations:

$$\Pi_u \rightarrow \begin{cases} (6s\sigma_g)^2 \quad (6p\sigma_u)(6d\Pi_g) \\ (6s\sigma_g) \quad (6p\sigma_u)^2(6p\Pi_u). \end{cases}$$

Either of these configurations would suggest an essentially repulsive potential curve, although a small well at large internuclear separation, as may be implied by the spectroscopic data, cannot be ruled out.

Finally, we must describe the spin sublevels and in particular the spin-orbit splittings. They are expected to be quite large in Hg_2. In the separated atom limit we observe that the Hg(6s6p) configuration decomposes to the various fine structure sublevels (in Russell-Saunders notation) $^1P_1$, $^3P_0$, $^3P_1$, $^3P_2$. In forming the Hg_2 molecule we note that each of these atomic sublevels produces a mixture of Σ and Π components when projected onto the internuclear axis. Of course in the molecule, the atomic angular momentum is no longer conserved, only the internuclear projection. As the Hg_2 molecule is formed, the p orbital uncouples from the spin and couples instead with the internuclear axis. The states make a gradual transition from Hund's cases (c) and (d) to cases (a) and (b). When this transformation is completed at small R, we can then refer to the states as $^3\Pi_2$, $^3\Pi_1$, $^3\Pi_{0^+}$, $^3\Pi_{0^-}$, $^1\Pi_1$, $^3\Sigma_1$, $^3\Sigma_{0^-}$, $^1\Sigma_{0^+}$. For more details about the fine structure of molecular states see Herzberg (ref. 5, Chapter V).

Decomposing the ^3P_J and $^1P_1$ levels into their Σ and Π components allows us to set up the matrix Hamiltonians to be diagonalized. These are shown in Table I. We use the notation of Condon and Shortley,[11] where ζ is the spin-orbit splitting parameter, G is the singlet-triplet splitting parameter, and W is a new parameter to designate the Σ-Π splitting. To calculate the relative energies of the molecular fine structure levels using the atomic parameters, we must assume that the spin-orbit interaction does not change drastically as a result of molecular distortion. These changes are probably small enough for the range of internuclear distance under consideration, and in particular the changes should be smooth enough that our qualitative view of the ordering of the states will remain applicable.

Figure 2 shows the relative energies of the fine structure levels of Hg_2 arising from Hg(6s6p) on Hg($6s^2$). The ordering and approximate energy separation of the states are shown as a function of the Σ-Π splitting energy. The Σ-Π splitting itself is expected to vary with R approximately as the overlap of one atom with the other, or about exponentially. As discussed above, we expect the Π_g states to be lower than the Σ_g states; hence the Σ-Π splitting is taken to be negative. Correspondingly the Π_u states should be higher than the Σ_u states, and in that case the splitting is positive.

Combining the information gained above from the correlation diagram (Figure 1) and the fine structure splittings (Figure 2), we are able to sketch a molecular energy diagram for Hg_2, which is presented in Figure 3. It must be remembered that this figure has been assembled from qualitative information. It is intended to give a plausible description of the states, and it is hoped that it can serve as a basis for comparing experimental and theoretical results.

Table I

MOLECULAR FINE STRUCTURE MATRICES FOR SP OR P^5S ATOMIC CONFIGURATIONS

O^-	$^3P^0_0$	$^3P^0_2$
$^3P^0_0$	$\frac{W}{6} - G$	$\sqrt{\frac{2}{9}}\, W$
$^3P^0_2$	$\sqrt{\frac{2}{9}}\, W$	$-\frac{W}{6} + \frac{\zeta}{2} - G$

O^+	$^1P^0_1$	$^3P^0_1$
$^1P^0_1$	$\frac{W}{2} + G$	$\sqrt{\frac{1}{2}}\, \zeta$
$^3P^0_1$	$\sqrt{\frac{1}{2}}\, \zeta$	$\frac{W}{2} - \frac{\zeta}{2} - G$

1	$^3P^1_2$	$^3P^1_1$	$^1P^1_1$
$^3P^1_2$	$\frac{\zeta}{2} - G$	$-\frac{W}{2}$	0
$^3P^1_1$	$-\frac{W}{2}$	$-\frac{\zeta}{2} - G$	$\sqrt{\frac{1}{2}}\, \zeta$
$^1P^1_1$	0	$\sqrt{\frac{1}{2}}\, \zeta$	$\frac{W}{2} + G$

2	$^3P^2_2$
$^3P^2_2$	$\frac{W}{2} + \frac{\zeta}{2} - G$

SA-1925-34

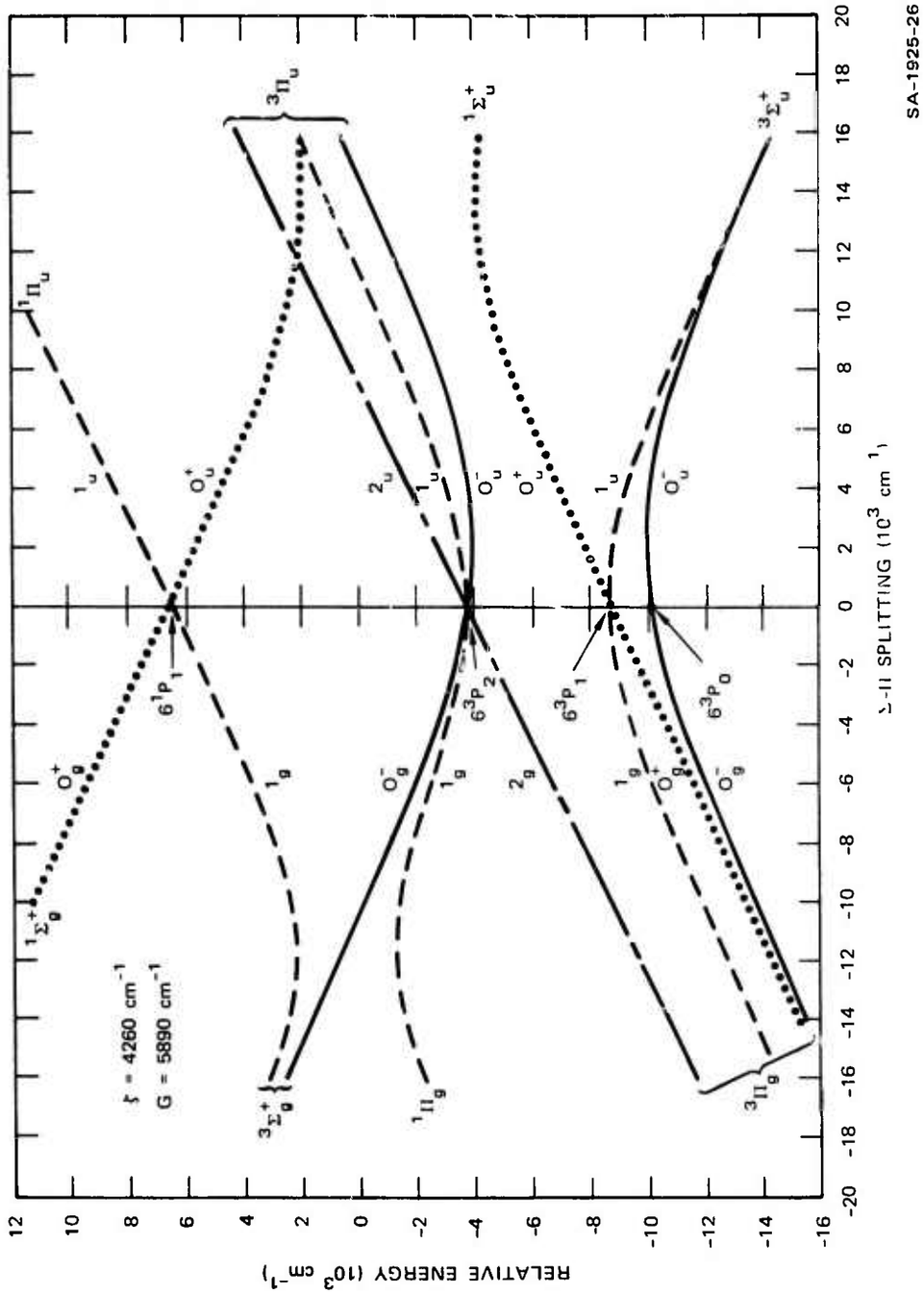

FIGURE 2 FINE STRUCTURE LEVEL DIAGRAM FOR Hg_2

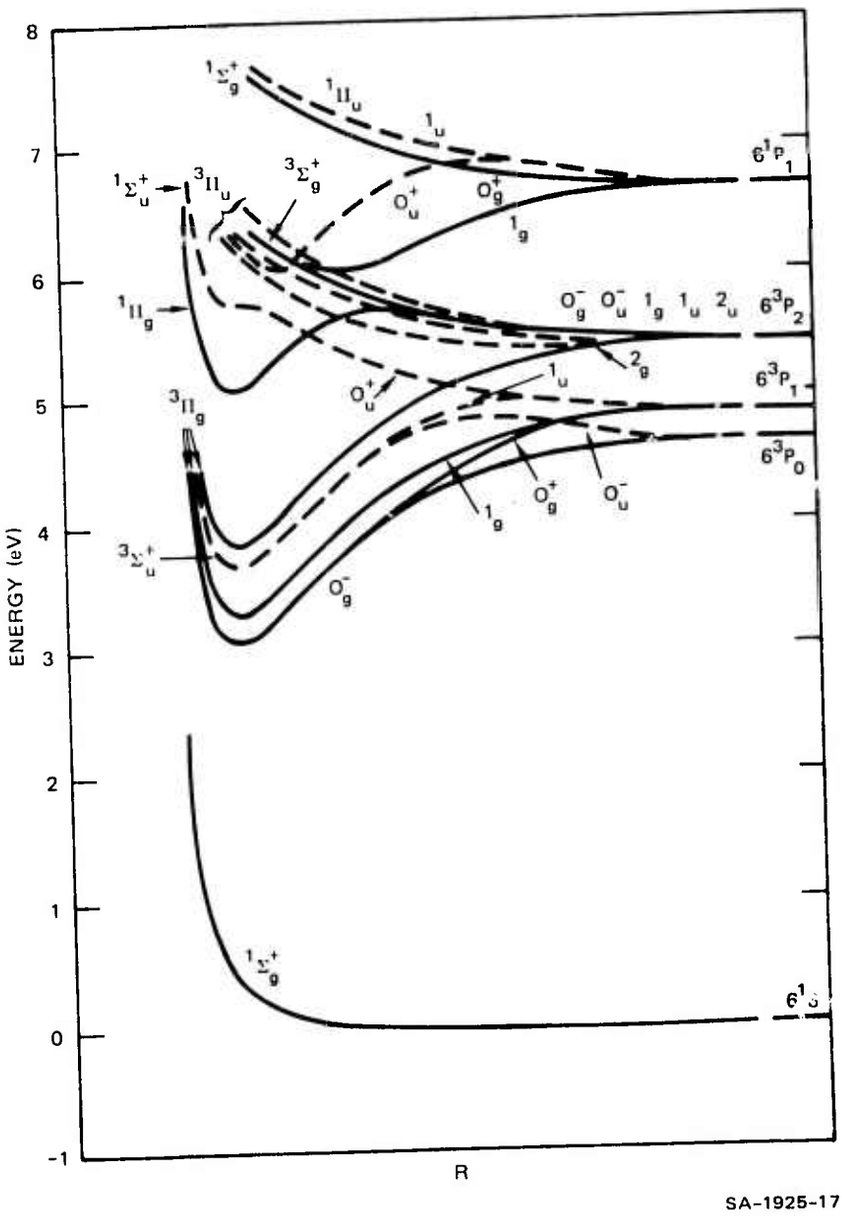

FIGURE 3 MOLECULAR ENERGY LEVEL DIAGRAM FOR Hg_2

Unfortunately the understanding of the mercury spectra has progressed rather little since Finkelnberg's review.[12] Indeed the level diagram presented in Figure 3 seems to introduce as much complication as clarification. However, certain important conclusions cannot be avoided:

(1) The spin-orbit splittings suggested in Figures 2 and 3 predict that the 0_u^- and 1_u components of the $^3\Sigma_u^+$ state should lie very close together at R_e, separated by approximately 200 cm^{-1}. Therefore they cannot separately be the upper states of the 4800 and 3300 Å bands.

(2) The humps predicted in the potential curves for the 0_u^- and 1_u states should have serious consequences for the kinetics of their formation.

(3) The $^3\Pi_g$ levels, formed without crossing energy barriers, will serve as reservoirs of excitation, which may subsequently be transferred into more rapidly radiating states. Their own radiative lifetimes should be quite long. In such a way all the emission bands would follow the decay of the reservoir and hence have the same lifetime.

(4) If the $^3\Pi_g$ levels do store a large fraction of the excitation, they may be the levels responsible for the absorption that results in the observed negative gain.

Obviously, there is much left to be understood, especially about the $^3\Pi_g$ states. No doubt the best sources of information about the $^3\Pi_g$ states will be metastable scattering experiments of the type of Morgenstern et al.,[13] further absorption measurements out of the excited $^3\Pi g$ states, and theoretical calculations.

III MIXED GASES

Introduction

The very great interest and attention that have been devoted to the possibility of lasing in van der Waals molecules have occurred because the lower state of the lasing transition is a dissociating repulsive state that is always essentially unpopulated. Thus a population inversion can readily be obtained on the continuum band resulting from these types of transitions, leading to the prospect of lasing that may even be continuously tunable over a wide frequency range.[1,2] To date, Xe_2[14] and Kr_2[15] have given conclusive evidence of laser action, but with apparent efficiencies well below those expected. We have been studying the excimer radiations from Hg_2 as part of this contract, and reported our results in Section II above. These earlier results have shown that photoabsorption of the excimer radiation can lead to decreased efficiency in the rare gas case and to negative gain (net absorption) in the case of Hg_2. The same studies also show that large concentrations of excimers in rare gases or metal vapors can be created with high efficiency and that interesting laser systems could be constructed if suitable ways of removing this energy could be found.

These considerations led us to consider the possibility of transferring the excitation produced in the excimer state into conventional molecular systems (i.e., bound-bound electronic transitions), which then can serve either as the laser medium itself or as an amplifier for an externally applied radiation signal. Additional motivation for exploring transfer systems arises from the following:

(1) Rare gas excimers radiate in the VUV, which does not appear to be as useful a region for medium to high power lasers as is the near-UV to visible range.

It is known that the transfer of energy from gas metastables to excited molecular states can be quite specific.[16] The transfer of excimer energy to molecular states may be equally specific, leading to the possibility of efficient pumping of a whole range of conventional laser transitions throughout the ultraviolet and visible.

(2) Because optical gain is inversely proportional to the transition linewidth, and because the continuum radiation resulting from excimer-repulsive transitions inherently has a large bandwidth, the gain in the dissociative-type transitions tends to be quite low. Thus a relatively high concentration of excimers is required to achieve threshold gain. However, if excimer energy can be transferred to molecules with bound-bound transitions that have very much narrower linewidths, then laser action can be achieved at much lower concentrations of excited states.

(3) In the field of laser induced fusion, a laser medium is required in which large amounts of energy can be stored to be released rapidly by amplifying an incoming pulse. This requires that the energy be stored in discrete levels and that the system be essentially metastable against radiative decay or quenching. The $N_2(A^3\Sigma_u^+)$ state is an interesting candidate for such energy storage and will be discussed in detail later in the report.

In following subsections, we discuss our approach to the transfer gas studies, the experiments, their results, and our interpretation of these results to date. We also discuss our kinetic modeling studies. Emphasis throughout is on the Ar + N_2 systems.

Our initial studies were made on argon plus small percentages of N_2. Ultimately, we will want to study many combinations of rare gases and transfer gas species, but the Ar + N_2 system has many advantages for the first experiment. First of these is that most of the reactions between these two systems have been studied, and rate constants for energy transfer and quenching of various states have been measured (see Table II). A second major reason is that the nitrogen triplet electronic states provide a good system for laser action as well as the capability for high energy storage. Lasing from the C and B states in N_2 (Second Positive: 2^+, C → B, and First Positive: 1^+, B → A radiation; see also Table III) has been demonstrated at moderate efficiency in discharges of pure nitrogen. Specific transfer of rare gas excimer energy into either C or B state N_2 could lead to efficient lasing on these transitions. The $A^3\Sigma_u^+$ states of N_2 is a well-known, long-lived, metastable state that does not interact significantly with rare gas atoms or with ground state N_2 molecules. This state, which is 6.2 eV above the ground state, should serve as a good energy storage reservoir. A third important reason for study of rare gas/N_2 mixtures is the considerable stability of the nitrogen molecule, compared with most other diatomic gases, both in its ground and excited states, against dissociation and reaction. The transfer from the rare gas excimers, specifically Ar_2^*, involves more energy than most molecules can contain without subsequent dissociation, ionization, or chemical reaction.

In following subsections, we discuss our experimental results for the excited triplet states of N_2 produced by Febetron excitation of Ar + N_2 mixtures (with and without a trace of NO) and show how the population and kinetics of these states can be determined, modeled, and understood.

TABLE II MIXED GAS REACTION SYSTEM ($Ar + N_2 + NO$)

Reaction No.	Reaction	Rate	Reference
Host gas reactions		Units: cm^3 sec or cm^6/sec	
1	$Ar^+ + 2\,Ar \rightarrow Ar_2^+ + Ar$	2.5×10^{-31}	a
2	$Ar_2^+ + e \rightarrow Ar^* + Ar$	7×10^{7}	b
3	$Ar^* + 2Ar \rightarrow Ar_2^* + Ar$	5×10^{-32}	c
4	$Ar_2^* \rightarrow 2Ar + h\nu$	1×10^{8}	d
5	$Ar_2^* + e \rightarrow 2Ar + e$	1×10^{-9}	Estimated
6	$Ar_2^* + Ar_2^* \rightarrow Ar_2^+ + 2Ar + e$	5×10^{-10}	Calculated
7	$Ar^* + Ar^* \rightarrow Ar^+ + Ar + e$	5×10^{-10}	Calculated
Added gas-host gas reactions			
8	$Ar^* + N_2(X) \rightarrow Ar + N_2(B)$	3×10^{-12}	e
9	$\rightarrow Ar + N_2(C)$	3×10^{-13}	f
10	$\rightarrow Ar + N_2^*$(unspecified)	5×10^{-11}	f
11	$Ar_2^* + N_2(X) \rightarrow 2Ar + N_2(B)$	1×10^{-11}	Guess
12	$N_2(C) + Ar \rightarrow N_2(B) + Ar$	1×10^{-13}	Guess
13	$N_2(B) + Ar \rightarrow N_2(A) + Ar$	1.6×10^{-12}	g
14	$N_2(A) + N_2(A) \rightarrow N_2(C) + N_2(X)$	2×10^{-11}	h
15	$\rightarrow N_2^* + N_2(X)$	3×10^{-10}	i
16	$N_2(C) \rightarrow N_2(B) + h\nu$	2.2×10^{7}	j, k
17	$N_2(B) \rightarrow N_2(A) + h\nu$	1.2×10^{5}	k
Secondary added gas reactions			
18	$N_2(A) + NO(X) \rightarrow N_2(X) + NO(A)$	8×10^{-11}	g, l
19	$NO(A) + Ar \rightarrow NO(X) + Ar$	1×10^{-13}	m, n
20	$NO(A) \rightarrow NO(X) + h\nu$	4.5×10^{6}	m
21	$NO(A) + NO(X) \rightarrow$ products	2×10^{-10}	n

TABLE II (CONCLUDED)

REFERENCES

a. E. W. McDaniel, et al., Ion-Molecule Reactions (Wiley-Interscience, New York, 1970), p. 338.

b. J. N. Bardsley and M. A. Biondi, in Advances in Atomic and Molecular Physics (Academic Press, New York, 1970), Chapter I.

c. E. Ellis and N. D. Twiddy, J. Phys. B 2, 1366 (1969).

d. H. A. Koehler, Lawrence Livermore Laboratory, private communication.

e. D. W. Setser, D. H. Stedman, and J. A. Coxon, J. Chem. Phys. 53, 1004 (1970).

f. R. A. Gutcheck and E. C. Zipf, Bull. Amer. Phys. Soc. 17, 395 (1972).

g. R. A. Young, G. Black, and T. G. Slanger, J. Chem. Phys. 50, 303 (1969)

h. D. H. Stedman and D. W. Setser, J. Chem. Phys. 50, 2256 (1969); E. C. Zipf, Bull. Amer. Phys. Soc. 10, 179 (1965).

i. E. C. Zipf, University of Pittsburgh, private communication.

j. J. E. Hesser, J. Chem. Phys. 48, 2518 (1968); A. W. Johnson and R. G. Fowler, J. Chem. Phys. 53, 65 (1970); J. M. Calo, R. C. Axtmann, and R. G. Persing, Rev. Sci. Instr. 41, 1639 (1970).

k. M. Jeunehomme and A.B.F. Duncan, J. Chem. Phys. 41, 1692 (1964).

l. A. B. Callear and P. M. Wood, Trans. Faraday Soc. 67, 272 (1971); R. A. Young and G. A. St. John, J. Chem. Phys. 48, 898 (1968).

m. A. B. Callear and I.W.M. Smith, Trans. Faraday Soc. 59, 1720 (1963).

n. H. P. Broida and T. Carrington, J. Chem. Phys. 38, 136 (1963).

TABLE III

WAVELENGTHS OF SELECTED N_2 and NO BAND SYSTEM EMISSIONS

Vegard-Kaplan:	$N_2(A^3\Sigma_u^+) \rightarrow N_2(X^1\Sigma_g^+)$		V-K
	(0-5)	2603.6 Å	
	(0-6)	2760.8	
First Positive:	$N_2(B^3\Pi_g) \rightarrow N_2(A^3\Sigma_u^+)$		1^+
	(0-0)	10,510.0 Å	
	(2-0)	7,753.2	
	(10-6)	5,854.4	
Second Positive:	$N_2(C^3\Pi_u) \rightarrow N_2(B^3\Pi_g)$		2^+
	(0-0)	3,371.3 Å	
	(0-3)	4,059.4	
	(1-0)	3,159.3	
Gamma Bands:	$NO(A^2\Sigma^+) \rightarrow NO(X^2\Pi)$		γ
	(0-3)	2586 Å	
	(0-4)	2712	
	(2-7)	2754	

Experiments

The experimental program continues to be centered on viewing the optical emissions resulting from the pulsed electron excitation of a gas mixture under high pressure. A Febetron 706 provides a 3-nsec, 7000-amp pulse of 500-keV electrons that enter the test cell through through a 1-mil Inconel foil. The test gas pressure is varied from 200 torr to 13,000 torr (or approximately 0.25 to 20 atm). The temporal behavior of the spectral emissions is examined by photographing oscilloscope traces (Tekronix models 555 and 485) of individual excitation pulses and then digitizing the recorded analog signal, using a CDC 6400 computer to produce labeled graphs. The general configuration remains the same as described in our first semiannual report[3] and is depicted schematically in Figure 4.

The stainless steel experimental cell used in these mixed-gas studies has a central body containing a 1-inch-diameter by 3-inch-long cavity and 0.5 inch-diameter by 3-inch-long sidearms. The electron-beam window (Inconel foil) is tangent to the 0.5-inch aperture of the sidearms. MgF_2 windows, sealed to the sidearms using Teflon gaskets, give us the capability of observing spectral emissions from 1300 Å to the infrared.

The energy transfer studies of the Ar-N_2 mixtures have required us to study both the 1^+ and 2^+ systems of N_2. The 1^+ band system was monitored by a filtered photometer, which viewed the $(B^3\Pi_g - A^3\Sigma_u^+)$ 0-0 transition at 10,510 Å. A mirror that reflected the optical signal by 90^0 was used to remove the photomultiplier tube (PMT) from any direct line stimulation by Febetron-produced x-rays. The visible and ultraviolet measurements were made utilizing both a narrow band photometer system and a 1/2-meter grating spectrometer (McPherson Model 216.5) with an S-5 response PMT (RCA 1P-28).

In our energy transfer studies, we have found that the impurity

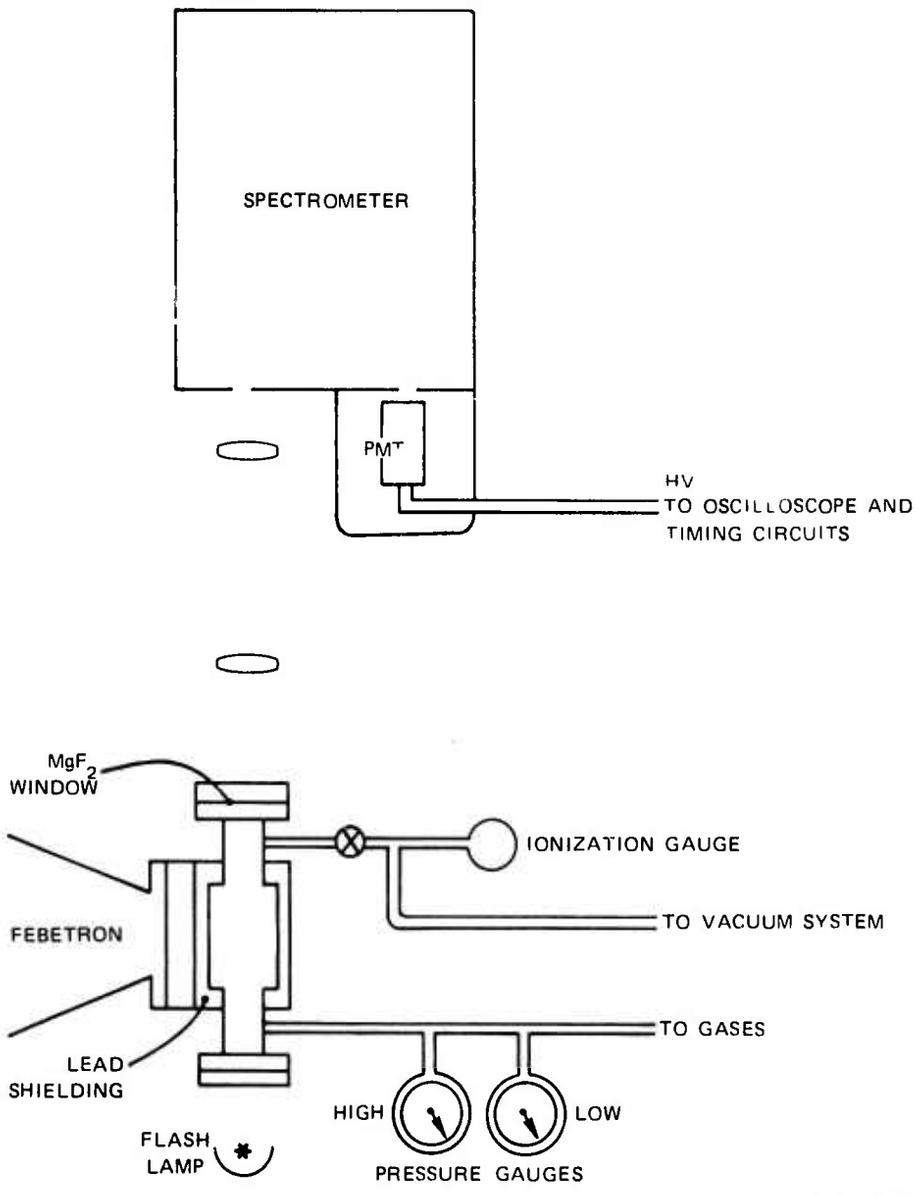

FIGURE 4 SCHEMATIC DIAGRAM OF APPARATUS

level in the experimental chamber can affect the temporal behavior of the spectral decays. An ionization gauge installed next to the cell has indicated that the residual impurity level in our diffusion pump-liquid nitrogen trap vacuum system is at the 0.1 ppm level for gases at 1 atm, much less than the impurity level inherent in the gases themselves. Nevertheless, in searching for Vegard-Kaplan radiation from N_2, we observed strong emission from the NO γ bands. The magnitube of the NO emission was found to be proportional to the number of electron pulses fired into any particular gas sample, leading to the conclusion that the N_2 excited by the pulse was reacting with O_2 that was present as an impurity in the test gas. Since the NO γ-band radiation is known to be a good tracer of $N_2(A)$ state population,[17] in most subsequent tests small amounts of NO were purposely added to the gas mixture. It was then found that the amount of NO decreased with repetitive electron excitation. Because transfer to even very small fractions of NO can be the dominant loss mechanism at very long times for $N_2(A)$ states, it was essential to know the concentration of NO accurately in order to produce repeatable data. Therefore, after each shot the cell was pumped out and a new volume of gas, (with a measured admixture of NO) was admitted before the next excitation pulse occurred.

For a reasonable signal-to-noise ratio, our method of measuring the long time decays ($\tau > 1$ μsec) forced us to saturate the PMT at early (20 nsec) periods of the decay. We feel, however, that the PMT had recovered from the saturation by the time that our data analysis began. We base this on the following observations:

(1) As we increased the signal by factors of 2, the intensity of the long tail increased also by a factor of 2.

(2) No discontinuity and no change of slope was observed as we increased the total signal from below to above saturation.

(3) When the PMT was operated in a pulsed mode, i.e. the voltage to the first dynode was pulsed on and off, the same observation held. The pulsed mode of operation, however, proved to be impractical because: the design of the pulsed mode circuitry permitted a large amount of ringing in the tube both at turn on and turn off of the voltage, the manner of operation cut down the gain by a factor of 5 in the "on" position, and the nonpulsed system provided for more flexibility in our measurements.

Summary of Experimental Results

Our experimental data consists primarily of a large number of time-resolved intensity histories of various spectral emission features as a function of pressure and gas mixture composition. We have concentrated thus far on measurements of the 1^+ and 2^+ bands of N_2 and the γ band of NO. In addition to the time-resolved results, we have taken some time-integrated (photographic) spectra.

Figure 5 shows some typical oscillograph traces of 1^+ and 2^+ intensity histories for Ar + 1% N_2 at 760 torr. Note that the 1^+ radiation starts promptly at the end of the excitation pulse, while the 2^+ intensity shows a slower buildup time, which we find varies inversely with the pressure. Figure 6 shows the long-time decay of the 3371 Å band in greater detail. It was assembled from four different oscillographs, taken at different times after the excitation pulse, but otherwise under the same experimental conditions. This figure gives an overall picture of the decay characteristics for the second positive radiation at medium pressure. One can see that a simple exponential decay does not fit these data except at long times.

Results such as those shown in Figures 5 and 6 are analyzed and

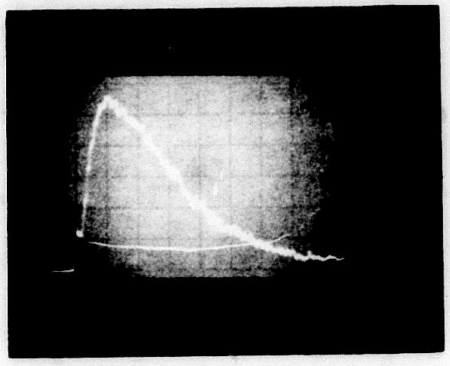

(a) SECOND POSITIVE BAND, $v' = 0 \rightarrow v'' = 0$, $\lambda = 3371$ Å

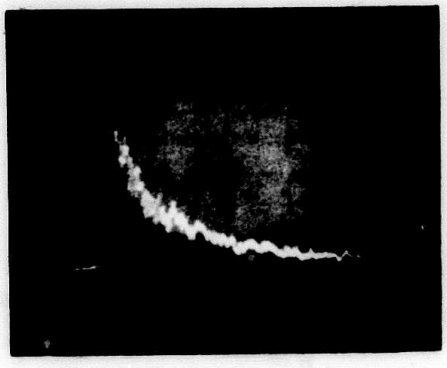

(b) FIRST POSITIVE BAND, $v' = 0 \rightarrow v'' = 0$, $\lambda = 1.05\ \mu$

SA-1925-31

FIGURE 5 TIME HISTORIES OF N_2 TRIPLET RADIATION FROM AR + 1% N_2 MIXTURE FOLLOWING 3 nsec EXCITATION PULSE

(Both photos: p = 760 torr, time scale 50 ns/cm)

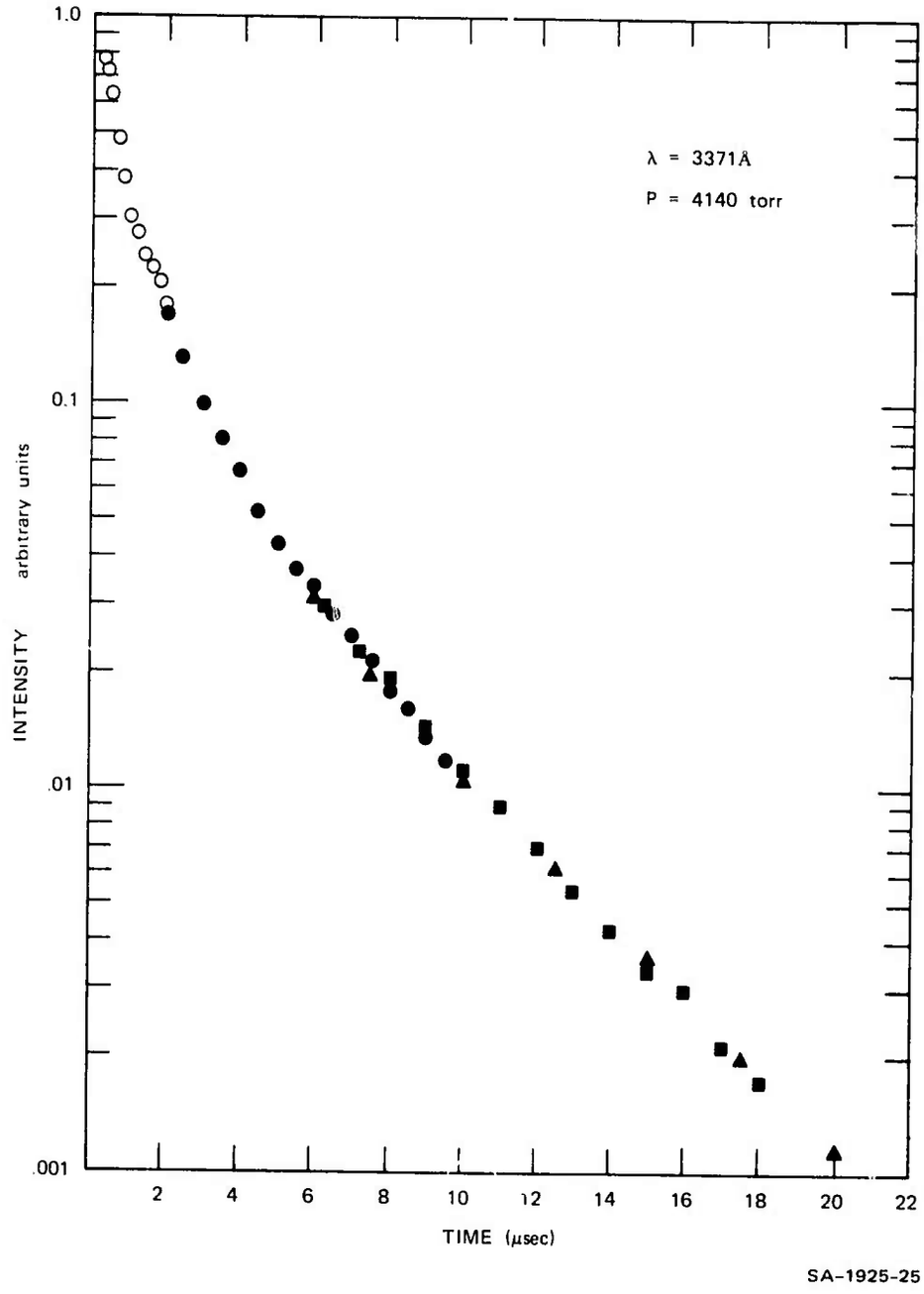

FIGURE 6 TIME DECAY OF N_2 SECOND POSITIVE EMISSION FOR 0.001% NO AND 1.05% N_2 IN ARGON

interpreted in the following subsection. To set the stage for that discussion, we can summarize our observations qualitatively as follows:

(1) Bright emissions are observed in the C → B 2+ and B → A 1+ systems. Most of this energy is contained in the first two or three vibrational levels of the upper states, with the greatest intensity appearing in the 0-0 transitions. Vibrational and rotational temperatures both appear to be low, with some evidence of rotational heating as a function of time after the electron beam excitation. The first and second positive systems appear to have "similar" intensities.

(2) The 2+ has a buildup time that is a function of pressure followed by a complex pressure-dependent decay. The 1+ radiation starts promptly at the end of the excitation pulse and has a complex decay behavior closely related to that of the second positive system. We believe the later part of this complex decay can be explained in terms of known molecular kinetics and that the derived rate constants agree reasonably well with accepted values.

(3) Quantitative values for the A state population as a function of time can be obtained from a combination of second positive radiation kinetics and the use of small amounts of NO as an impurity. The NO impurity (which reacts with the $N_2(A)$ state) gives rise to the γ band NO(A)-NO(X) radiation.

(4) The overall behavior of the pulse-excited Ar + N_2 mixture agrees reasonably well with the modeling (to be described in a later subsection) and we believe that the overall kinetics, energy deposition, and energy transfer in this system can be understood.

Analysis

In the excitation of the two-component gas mixture of Ar-N_2, we observed a large energy transfer rate from the argon excimers to N_2, resulting in intense emissions of the 1+ and 2+ systems of N_2. The resulting decay of these bands suggests that the energy transferred to N_2 does not merely filter to the lowest levels by radiation and quenching, but that at least part of the energy is recycled within the triplet system and reappears as radiation far later in time would have been expected.

To interpret these results we need to describe a plausible scheme for the energy deposition, transfer, and decay. This scheme, which will be discussed in greater detail in the modeling section that follows, is outlined in Figure 7.

We will divide our analysis into two temporal parts: early times of less than 1 μsec after the excitation pulse, and longer decay times of 1 to 20 μsec. Because of the short (45 nsec) radiative lifetime of the $N_2(C^3\Pi_u)$ state, the 2+ emissions serve as a convenient monitor of the decay of whatever species is serving as the energy reservoir. The decay frequency during the initial part of the afterglow as a function of total pressure is shown in Figure 8. The power law relation between the 2+ system and the total pressure is 1.2 ± 0.1. Notice that the initial decay is unaffected by the partial pressure of N_2, and that the same behavior is observed for both the $v = 0$ and $v = 1$ vibrational levels of $N_2(C)$. A similar result was obtained for the 1+ emission as displayed in Figure 9. Two features are worth noting. Although there is considerable scatter, the decay times for the two systems are essentially the same for any given pressure, and the decay rates are nearly proportional to pressure. A best fit through these data, directly proportional to the pressure, would give a rate constant for the quenching of the excited state. This rate

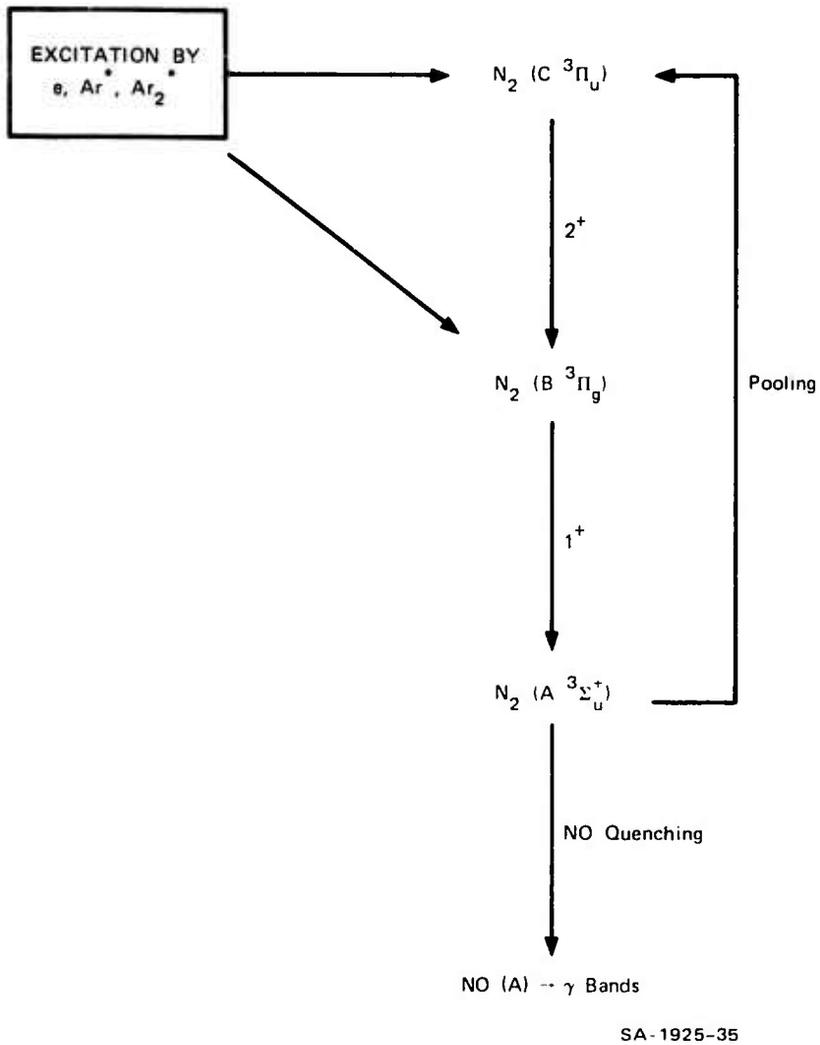

FIGURE 7 SCHEMATIC DIAGRAM OF $Ar/N_2/NO$ ENERGY FLOW

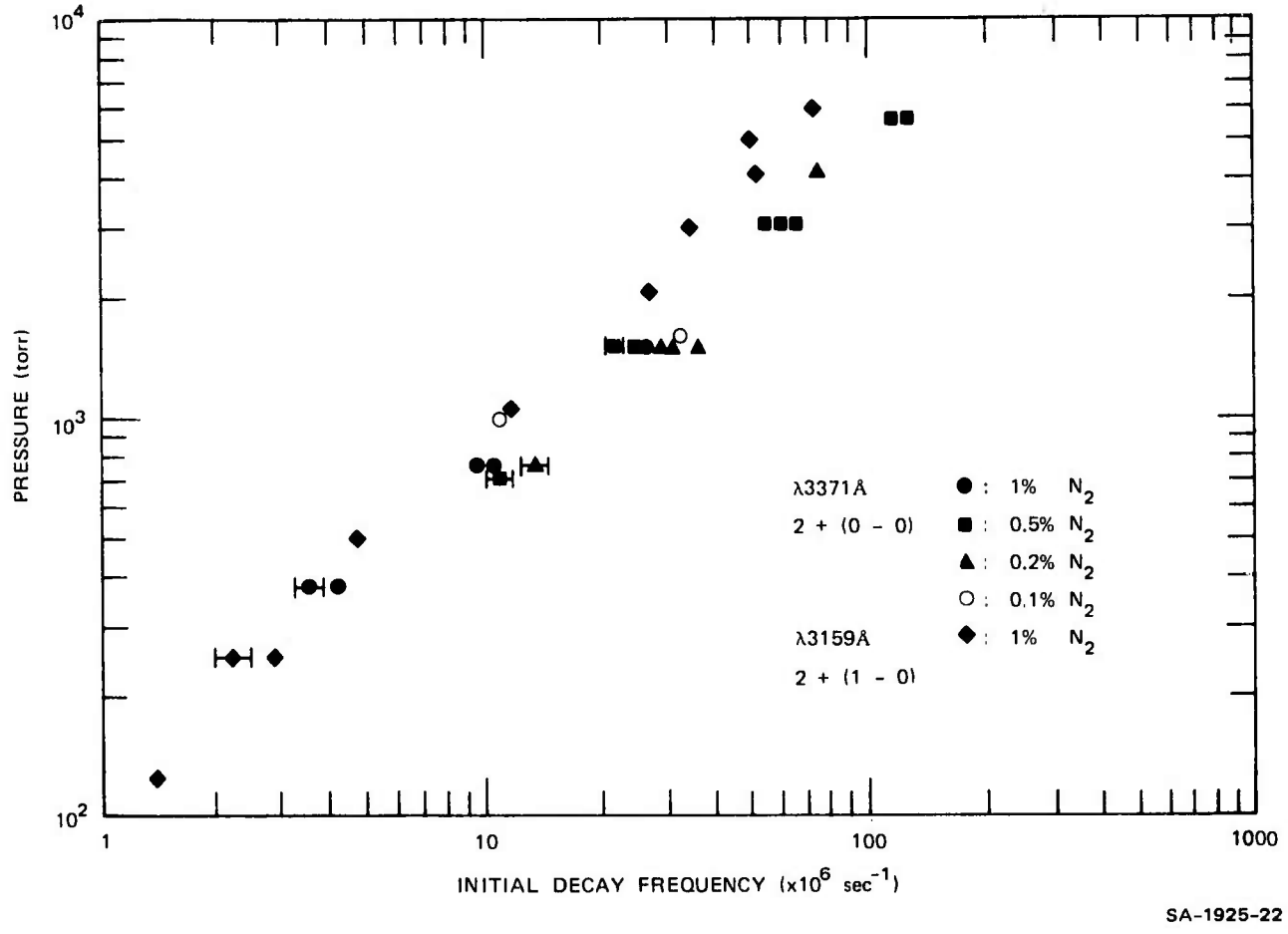

FIGURE 8 N_2 SECOND POSITIVE INITIAL DECAY FREQUENCY VERSUS TOTAL PRESSURE FOR VARIOUS CONCENTRATIONS OF N_2 IN ARGON

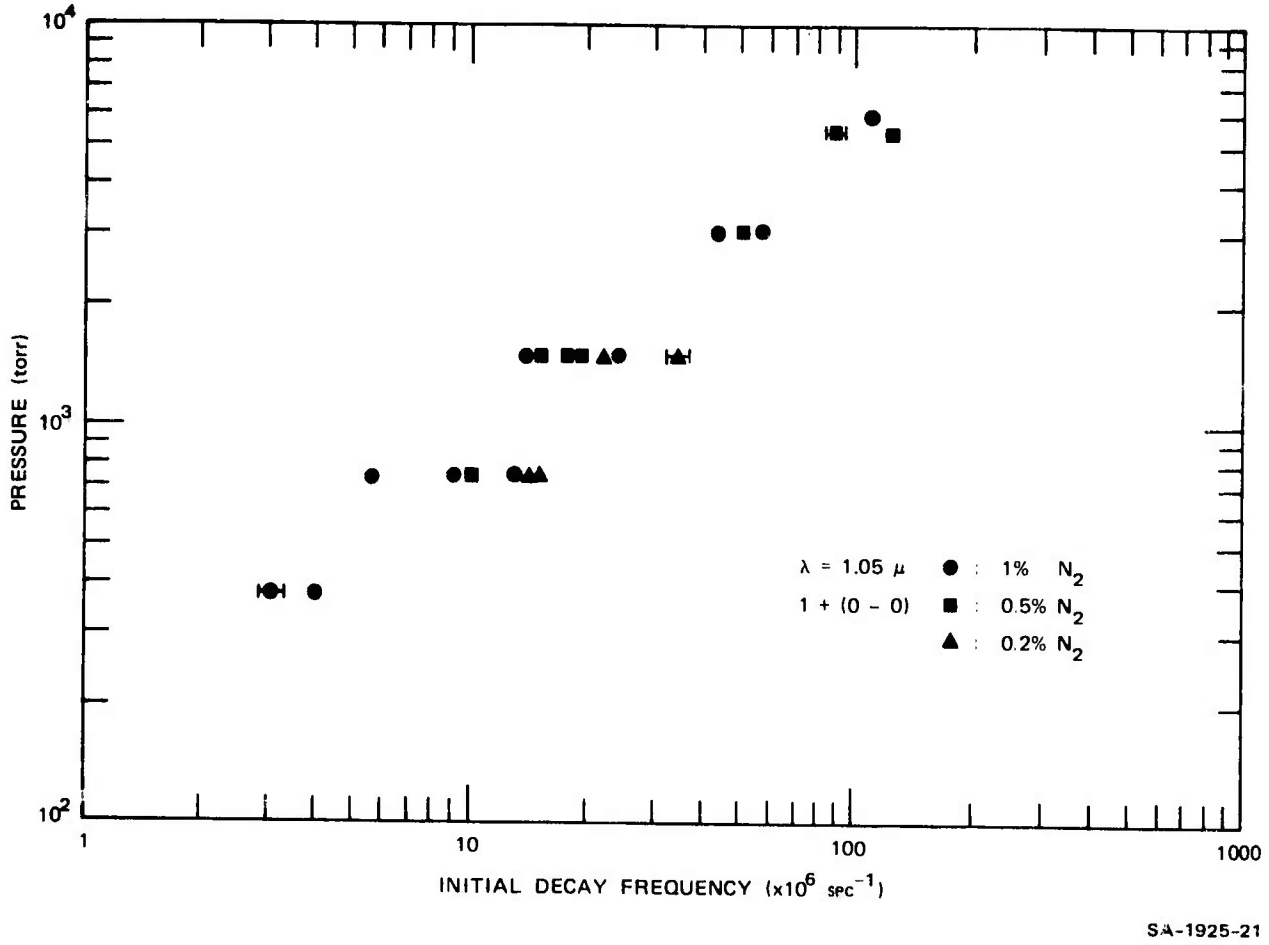

FIGURE 9 N_2 FIRST POSITIVE INITIAL DECAY FREQUENCY VERSUS TOTAL PRESSURE FOR VARIOUS CONCENTRATIONS OF N_2 IN ARGON

constant is ~4 x 10^{-13} cm^3/sec, which is between those for quenching of the nitrogen B and C states by argon (reactions 12 and 13, Table II). We do not understand at this time why the observed decay constants for the C and B states should be so similar. In particular it is remarkable that at pressures less than 1000 torr the 2+ radiation should decay with a lifetime longer than its own radiative lifetime. A plausible guess might be that the metastable $N_2(E^3\Sigma_g^+)$ state is serving as a reservoir for the early time 2+ and 1+ emissions.

Figure 15 in the modeling section below also illustrates the complexity of the very early time behavior. Detailed comparisons of the time behavior of first and second positive radiation as well as measurements of the time history of the Ar_2^* ultraviolet continuum will allow us to get a better understanding of the important kinetics for this part of the reaction period.

At later times after the excitation pulse the 2+ decay rate is two orders of magnitude slower than its radiative decay rate (reaction 16). The upper radiating level, the C state, is therefore being generated by yet another source. The most plausible candidate is the collision of two $N_2(A)$ excimers (reaction 14). Since the radiative decay rate is short compared with the production rate, the density of C should then be proportional to $[N_2(A)]^2$ and should have an apparent decay rate equal to twice that of the $N_2(A)$ state. To verify this and to get a measure of the A state population itself, we added trace amounts of NO and studied γ-band radiation, $NO(A \rightarrow X)$, as an indicator of the $N_2(A)$ population (reaction 18).

Figure 10 shows a typical plot of the observed γ-band intensity versus time. We found that the introduction of NO, even at the 0.001% level, caused both the 2+ and the γ-band emissions to become exponential in the very late decay periods. The observed final decay frequency of the NO γ bands varied as a function of both total pressure and

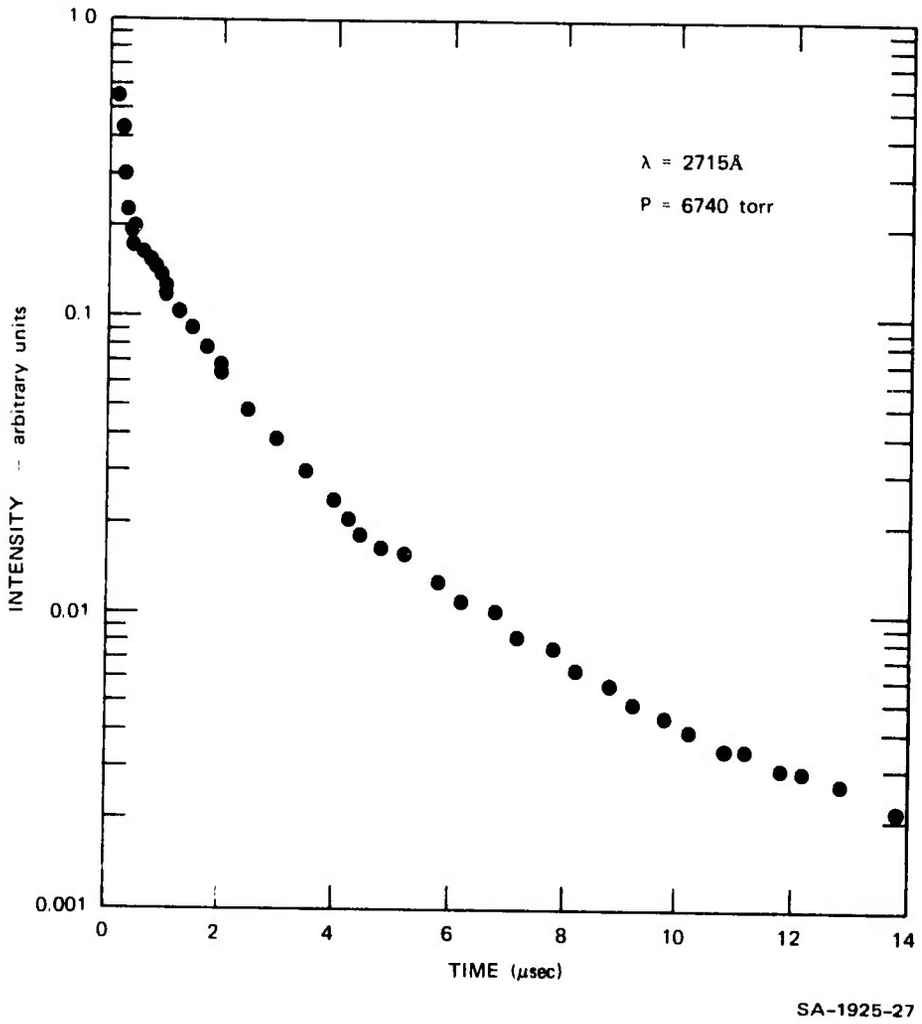

FIGURE 10 TIME DECAY OF THE NO γ-BAND EMISSION FOR A MIXTURE OF 0.001% NO AND 1.05% N_2 IN ARGON

partial pressure of NO (Figure 11) while the rate coefficient computed from NO decay ($10 \pm 3 \times 10^{-11}$ cm^3/sec) was found to be within statistical error the value accepted for reaction 18, indicating that NO quenching had become the dominant loss term affecting the $N_2(A)$ population.

Figure 6 above shows the intensity decay of the 2+ signal at later times. It becomes exponential quite far into the decay (~9 μsec), reflecting once again that the $N_2(A)$ decay is finally being controlled by NO quenching. The slope obtained from the exponential part of the decay is twice as large as the one expected for NO quenching of $N_2(A)$. Since $N_2(C)$ is produced by a reaction quadratic in $N_2(A)$ (reaction 14), a linear loss rate of $N_2(A)$ will appear to be twice as large in the $N_2(C)$ decay. Our measured rate coefficient from the $N_2(C)$ decay ($9 \pm 2 \times 10^{-11}$ cm^3/sec) agrees with that found above

The early nonexponential part of the 2+ decay in Figure 6 and the NO γ-band decay in Figure 10 indicate that both quadratic and linear loss mechanisms are contributing in this time period. We expect the $N_2(A^3\Sigma_u^+)$ population to obey a differential equation of the same form as the one for the mercury excimer discussed in our previous semi-annual report.[3] Specifically, for longer times

$$A' \approx -K_q A - K_p A^2$$

The quenching constant K_q is due mostly to quenching by NO (i.e. reaction 18 as illustrated above), and K_p is the excimer-excimer annihilation constant (reaction 15).

In our earlier work we found both the formal solution to this

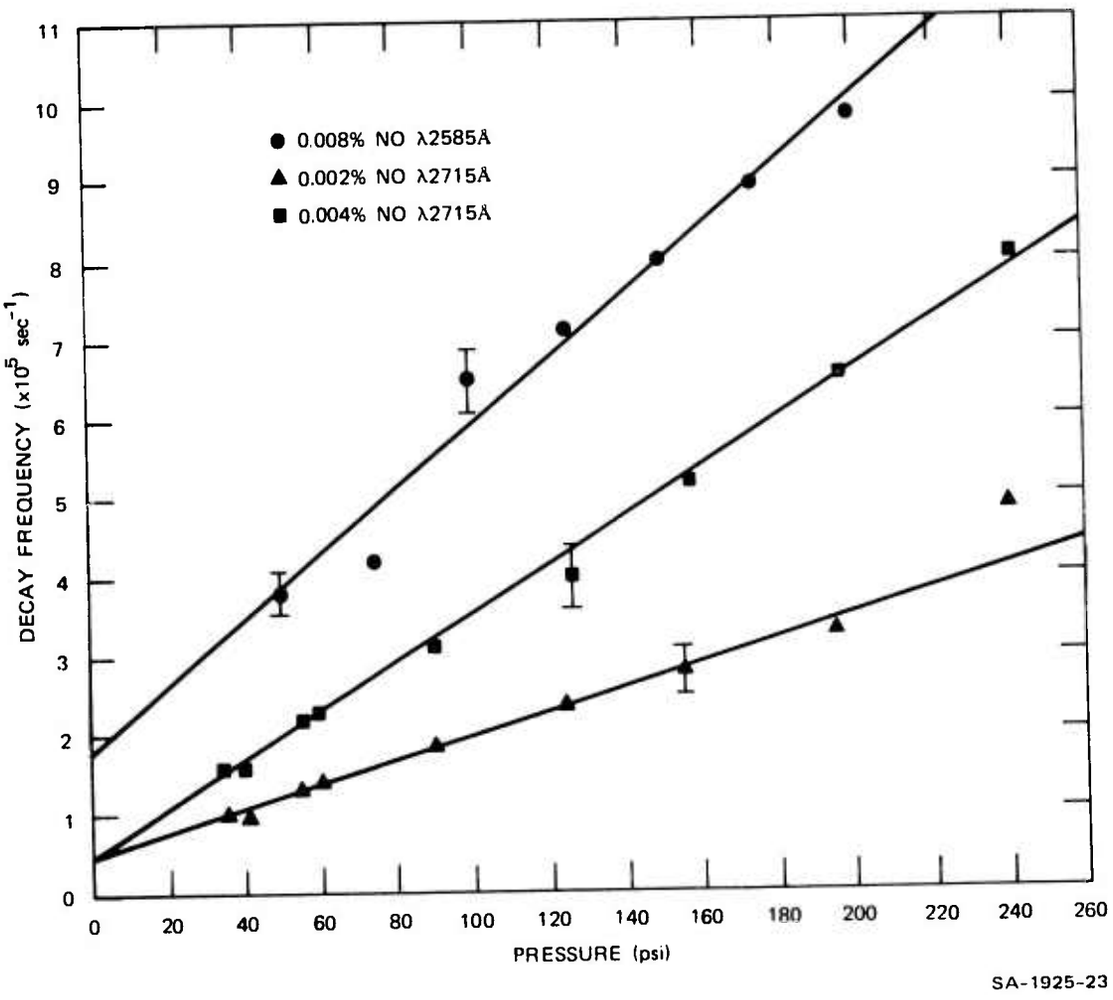

FIGURE 11 FINAL DECAY FREQUENCY OF THE NO γ-BAND EMISSION VERSUS TOTAL PRESSURE FOR VARIOUS CONCENTRATIONS OF NO IN A 1% N_2/Ar MIXTURE

decay equation and its various asymptotic limits. For all times the formal solution is

$$A = \exp(-K_q t)\left[\left(\frac{K_p}{K_q} + \frac{1}{A_o}\right) - \frac{K_p}{K_q}\exp(-K_q t)\right]^{-1}$$

where A_o is the population of $N_2(A)$ at time zero. At early times this has the asymptotic form.

$$A \sim \frac{A_o}{1 + K_p A_o t},$$

and at late times

$$A \sim \exp(-K_q t)\left(\frac{K_p}{K_q} + \frac{1}{A_o}\right)^{-1}.$$

The exponential behavior at long times has already been discussed. At shorter times, as noted in our previous report, a plot of 1/A vs t should give a straight line for a considerable range of t. We have already indicated that we expect the $N_2(C)$ population to be proportional to the square of $N_2(A)$. Hence a plot of $[C]^{-\frac{1}{2}}$ versus t should give a straight line. Such a plot is shown in Figure 12. The linear relationship that appears between 300 nsec and 9 μsec implies that the A state decay is indeed being controlled by the energy-pooling reaction 15, and that reaction 14 is the source of the $N_2(C)$ population.

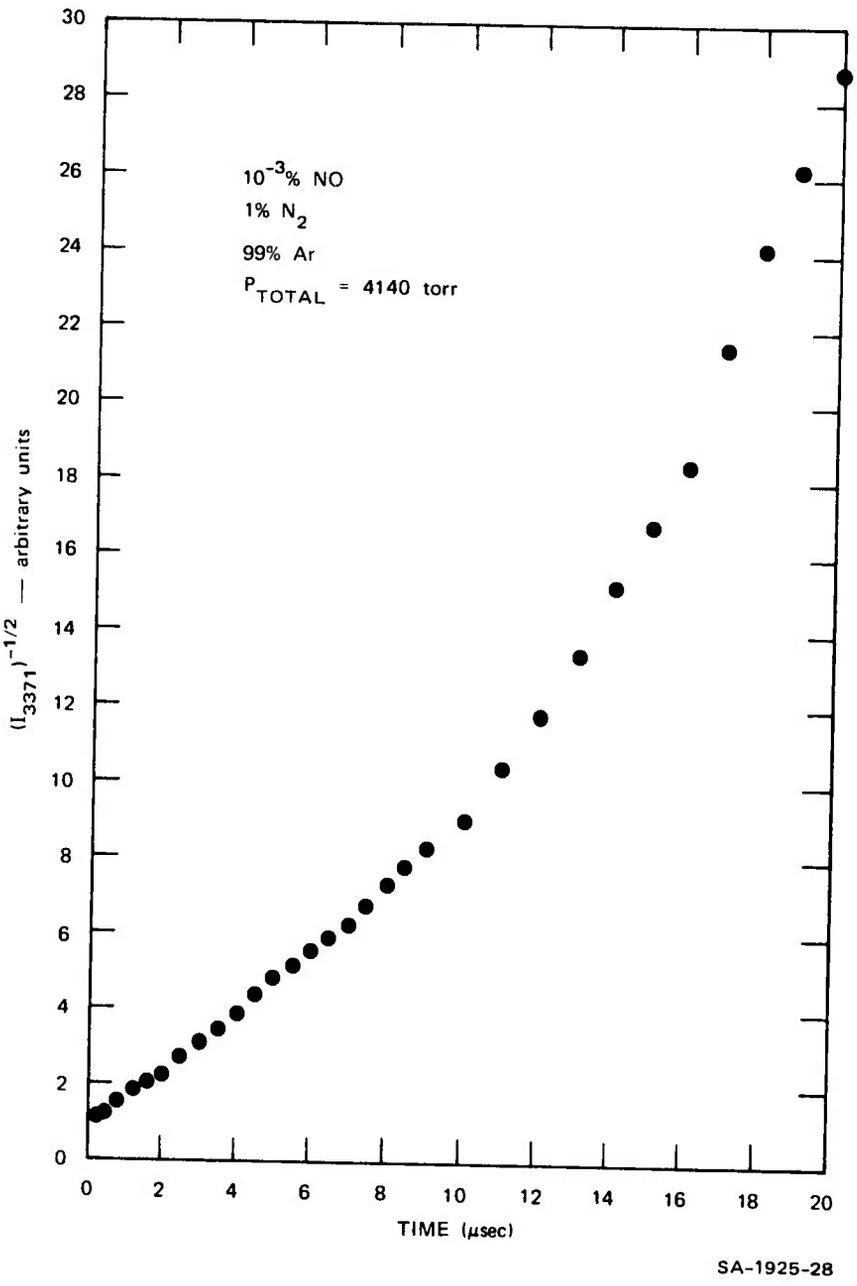

FIGURE 12 PLOT OF RECIPROCAL OF SQUARE ROOT OF N_2 SECOND POSITIVE INTENSITY VERSUS TIME

For longer times we rewrite the decay equation in the form

$$\frac{A'}{A} = -K_q - K_p A.$$

We see that a direct relationship ought to exist between the logarithmic derivative and the A state population. Figure 13 shows that this is indeed the case for both the NO γ bands and the N_2 2+ bands. Again, the decay rate of $N_2(A)$ at some point in the decay is equal to the logarithmic derivative of the γ-band intensity and also to the logarithmic derivative of the square root of the second positive intensity. The value of the intercept is just K_q, or in our case just the linear rate of quenching of NO (reaction 18). By subtracting the intercept value from the total value of the logarithmic derivative at a given intensity, one obtains the product of the A state population and the energy pooling rate coefficient. We can then use Zipf's value for K_p (reaction 15) and determine the $N_2(A)$ population. Since each intensity along the abscissa has a time associated with it, we can plot the $N_2(A)$ population computed as a function of time after the excitation pulse (Figure 14). The densities so determined have the same time behavior and are within an order of magnitude of those derived from our model (see below).

To recapitulate we may note that a substantial portion of the excitation appears in the N_2 triplet system. It filters down to the $N_2(A^3\Sigma_u^+)$ state, which becomes the principal energy storage reservoir at later times. The $N_2(A)$ population decays by:

(1) Excimer-excimer annihilation, producing

$N_2(C) \rightarrow N_2(B)$ (second positive) and

$N_2(B) \rightarrow N_2(A)$ (first positive) emissions

(2) Quenching by NO, which results in NO γ-band emissions.

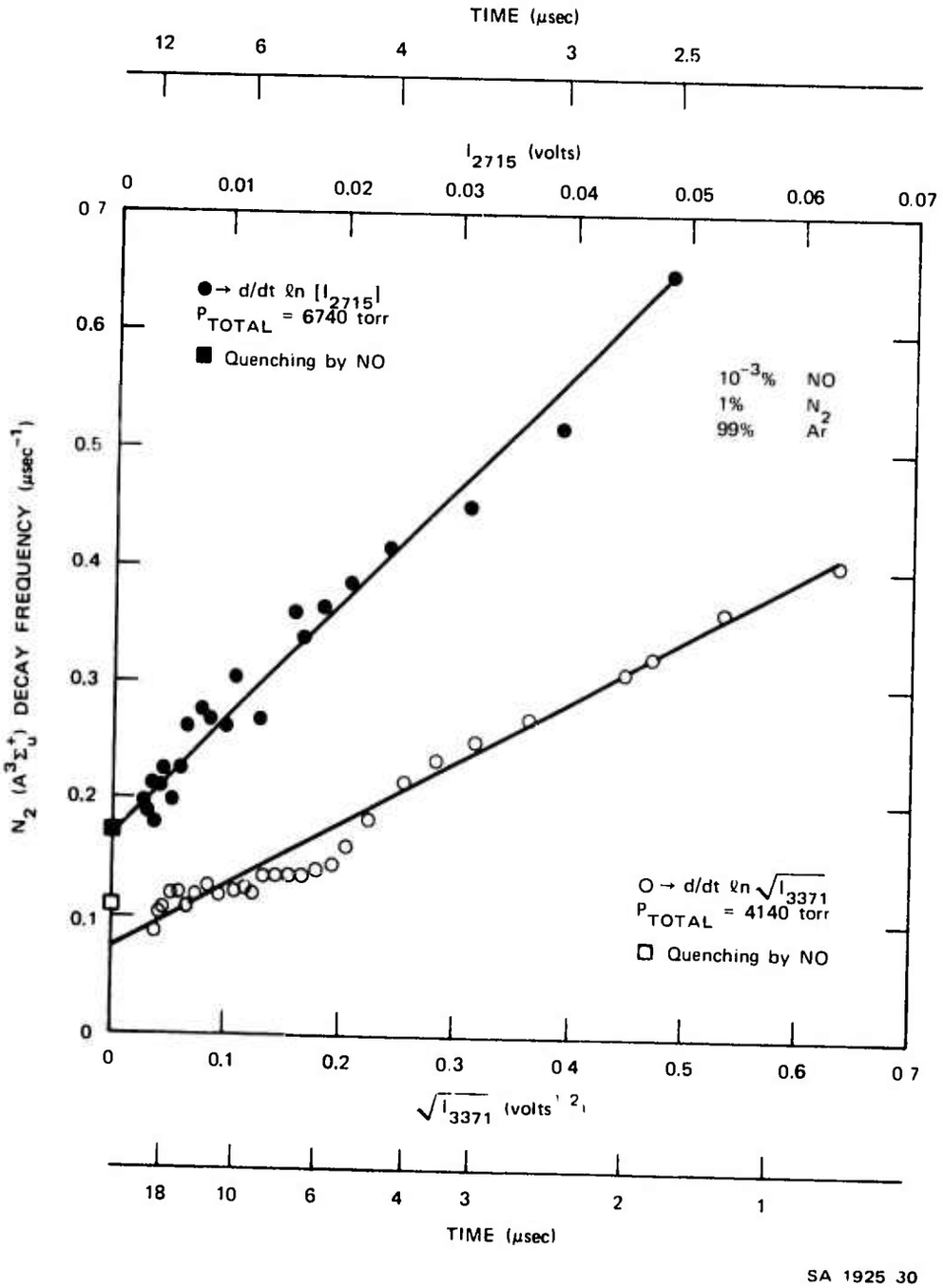

FIGURE 13 PLOT OF N_2 ($A^3\Sigma_u^+$) DECAY FREQUENCY AS COMPUTED FROM LOGARITHMIC DERIVATIVES OF N_2 SECOND POSITIVE AND NO γ-BAND INTENSITIES

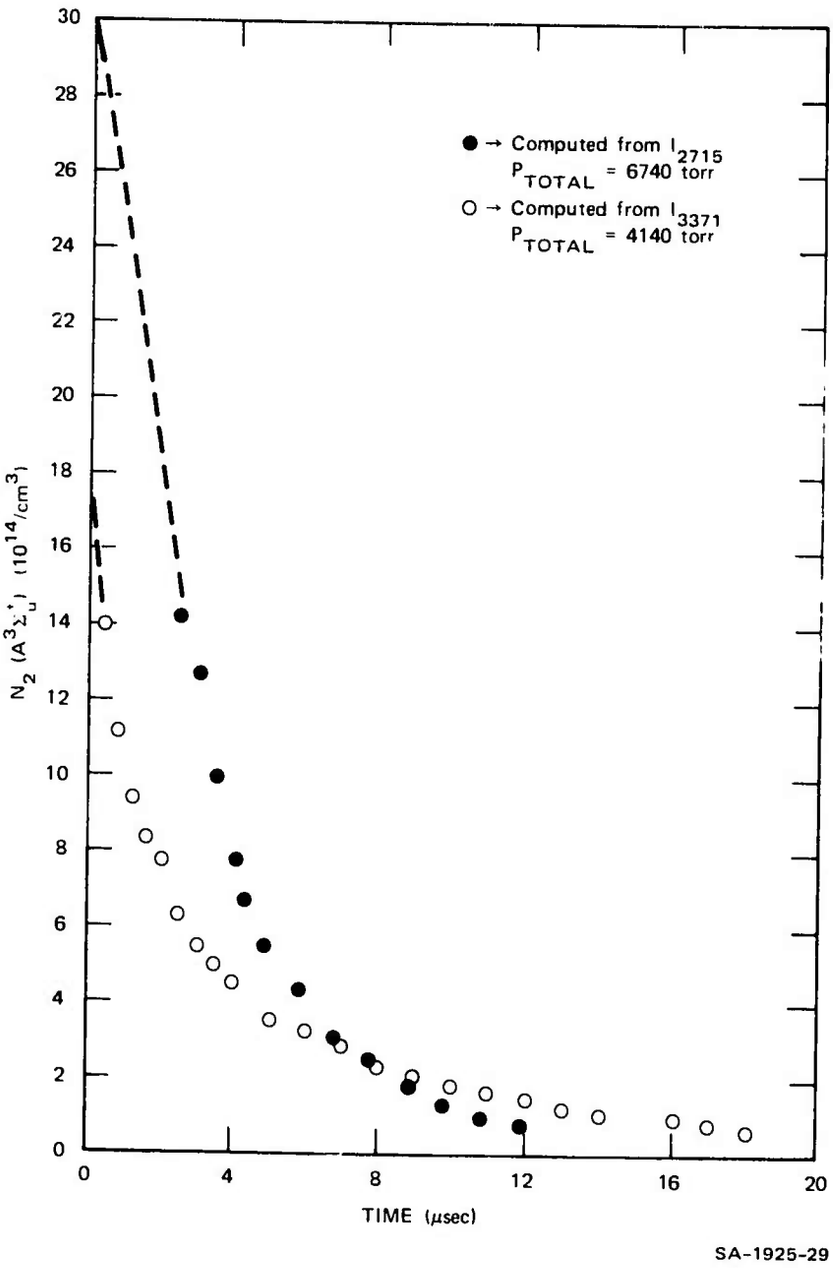

FIGURE 14 $N_2(A^3\Sigma_u^+)$ CONCENTRATION COMPUTED FROM ITS NONEXPONENTIAL DECAY

In particular, analysis of these emissions gives an estimate of the $N_2(A^3\Sigma_u^+)$ population (to be compared with model calculations discussed below), and can be used to design laser systems to release stored energy.

Modeling Studies

We have demonstrated in our studies of the rare gases and of mercury that understanding and interpreting experimental results is greatly enhanced by concurrent numerical modeling of the kinetics of the reaction system. Modeling will be even more important in the mixed-gas studies because of the greater number of reactions taking place. We have therefore modified the computer program that was used for the rare gases[18] and mercury, with specific application initially to the argon-N_2 system.

The earliest model of the pure gas system (e.g., argon) considered the atomic and molecular ions (Ar^+ and Ar_2^+), electrons (e), and the metastable atoms and molecules (Ar* and Ar_2*), as well as the ground state Ar atoms, in a seven-reaction system (reactions 1-7 of Table II). Subsequent pure-gas models have considered intermediate-level excited atoms and molecules, (Ar** and Ar_2**) with their attendant reactions, but the results of the more sophisticated model have not yet justified its additional computer costs for the mixed-gas studies. The basis for choosing (and limiting ourselves to) these seven reactions for the pure rare gases was described in detail in an earlier report.[18] That report also described the determination of the rates given in Table II. They are either known from measurements or can be reasonably well estimated.

In modifying the reaction model for gas mixtures, the situation is not so straightforward. The current form of the model for Ar + N_2 reported here considers the triplet (C, B, and A) excited

states of N_2 as well as the $N_2(X)$ ground state. These excited states were chosen because their energies are nearly resonant with those of the Ar* and Ar_2^* metastable levels, and because they can be more readily observed spectroscopically than the many other low-lying states in N_2. Indeed, they were observed to be strong emitters, as described above in the experimental section. In addition, because of the inevitable or intentional presence of NO (see the experimental section), we include the A and X states of NO. Since the A states of N_2 and NO are almost exactly resonant, the energy transfer between them is very rapid, and the γ-band radiation (A-X) of NO provides a convenient tracer for the $N_2(A)$ state population.

The reactions in this mixed-gas model include the nearly resonant energy transfer processes between Ar* and the C and B states of N_2, between Ar_2^* and $N_2(B)$, and between $N_2(A)$ and NO(A); quenching of $N_2(C)$, $N_2(B)$, and NO(A); and radiation from these same three states. We also consider the bimolecular reaction 14

$$N_2(A) + N_2(A) \rightarrow N_2(C) + N_2(X)$$

which plays an important role in populating the $N_2(C)$ state at long times after the electron pulse. All these reactions are listed in Table II, together with the rates we are currently using in our modeling studies. Most of these rates have been measured; only in the case of energy transfer from Ar_2^* to N_2 and of the quenching of $N_2(C)$ by Ar must we estimate them.

Although the Ar-N_2 system is the most studied of all mixed-gas systems, there are some important unanswered questions. For example, the known rate of energy transfer from metastable Ar* specifically into the $N_2(B)$ and $N_2(C)$ states (reactions 8 and 9 of Table II) is

substantially less than the total loss rate of Ar^*, which we have denoted as transfer into unspecified N_2^* states with the rate given for reaction 10, Likewise, the total rate for loss of $N_2(A)$ state in collisions with itself is substantially larger than the known production specifically into $N_2(C)$ state, as given by reactions 14 and 15. The rather large amounts of "unaccounted" energy may produce N_2^* states that have not been observed spectroscopically, or it may lead to dissociation of N_2 and production of N atoms. It may be important to the interpretation of our experimental results to deduce the paths of energy transfer in more detail, and it is likely, in particular, that N atoms will be included in the model in the near future. The rates for the $N_2(A)$ energy-pooling reactions 14 and 15 are crucial parameters, and we will try to verify them experimentally.

The computer program modifications required to include the additional species and reactions of a mixed gas system have been carried out. Some typical results for the case of 1% N_2 and 0.002% NO in Ar at 4 atmospheres total pressure are presented in Figure 15. The early times results show, primarily, the rapid conversion of Ar excitation to the $N_2(A)$ state, which then serves as an energy reservoir. The primary $N_2(A)$ population loss mechanism on a microsecond time scale is the $N_2(A) + N_2(A)$ reaction 15. At the NO concentration specified, the interspecies transfer constitutes a minor loss of $N_2(A)$ state, and the NO(A) population is seen to follow the $N_2(A)$ population, as suggested above. After 200 nsec, the only sources of $N_2(C)$ and $N_2(B)$ states are from the $N_2(A)$-$N_2(A)$ collisions. Since the former populations are proportional to $N_2(A)^2$, the final decay rates of $N_2(C)$ and $N_2(B)$ are twice that of $N_2(A)$, as seen also from Figure 15b.

Time has not yet permitted detailed comparison of the results predicted by the model with those obtained experimentally. Such

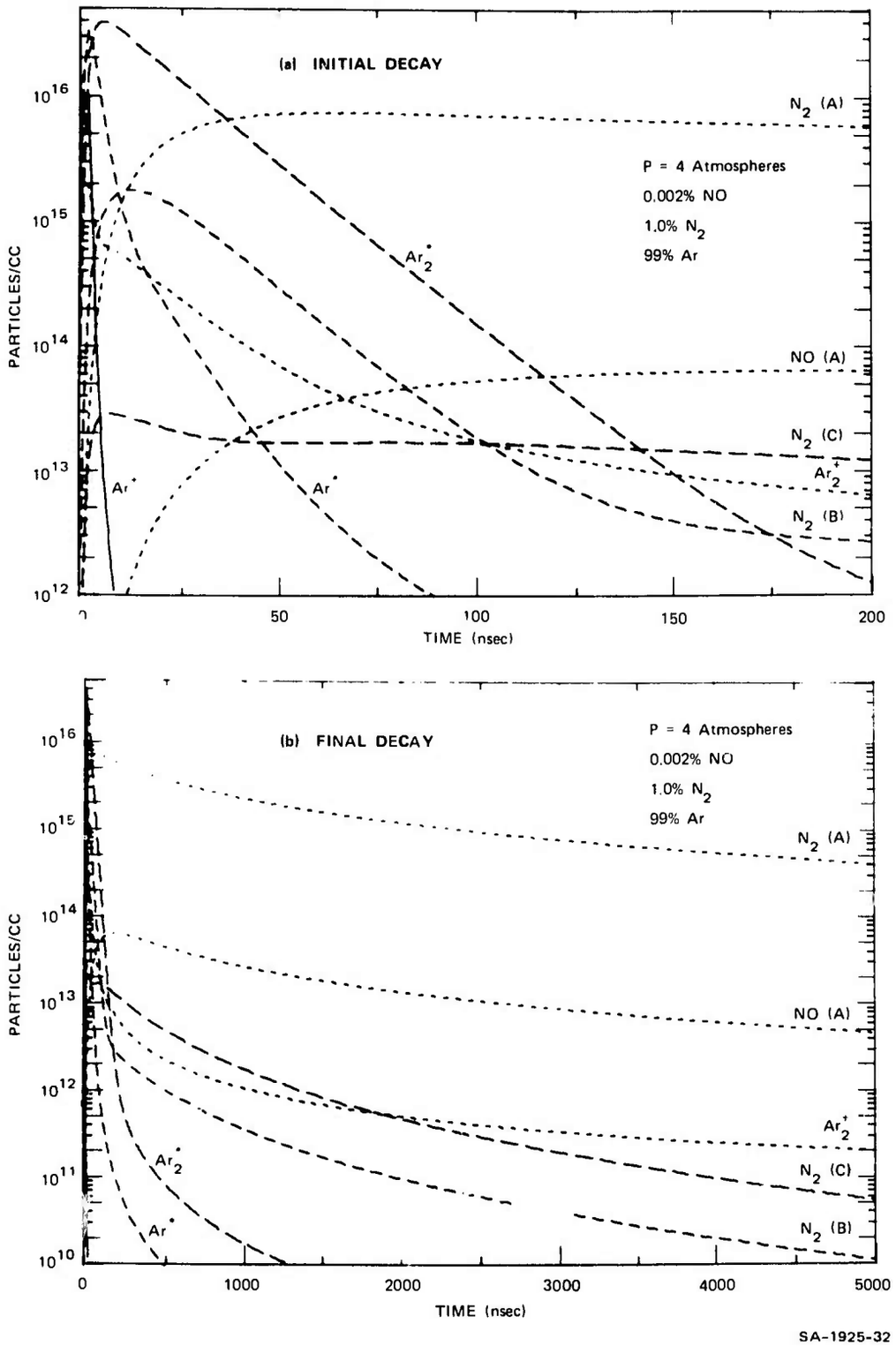

FIGURE 15 NUMBER DENSITIES OF VARIOUS SPECIES IN A FEBETRON-EXCITED NO-N_2-Ar MIXTURE VERSUS TIME AS DERIVED FROM MODEL CALCULATION

comparison will lead to modifications of the model and ultimately to a better understanding of this and other mixed gas systems.

IV CONCLUSIONS

Mercury Studies

The principal conclusions of our studies of excitation of high pressure mercury are:

(1) Both the 3350 and the 4800 Å continuum bands of Hg_2^* exhibit a radiative decay time of 14 ± 3 μsec, independent of pressure.

(2) The absorption cross section of Hg_2^* is larger than its stimulated emission cross section, resulting in a net absorption over the wavelength range from 3900 to 5145 A.

(3) We believe that the above result precludes the possibility of direct laser action in Hg_2, and we have therefore stopped our studies of pure Hg_2.

(4) High-pressure mercury remains an attractive candidate for energy storage and may serve as a host for mixed gas systems.

(5) We have presented in this report an outline of a new analysis of the state structure of Hg_2 that may lead to explanations for observed radiative behavior.

Mixed Gas Studies

Our studies of mixed gas systems have begun recently, and we have examined only the Ar + N_2 + NO system in any detail.

Our findings to date are:

(1) A substantial portion of the Ar excitation energy is transferred to the N_2 triplet states.

(2) After approximately 100 nsec, most energy resides in the $N_2(A)$ state. The decay of this state is governed by energy pooling reactions that lead to excitation of $N_2(C)$ and $N_2(B)$ states and by transfer to NO. The $N_2(A)$ population history can be determined from N_2 2+ and 1+ radiation as well as from NO γ-band radiation.

(3) The population histories of the N_2 and NO excited states appear to be in reasonable agreement with predictions made using our mixed gas kinetics computer program. Some discrepancies in early time behavior remain to be resolved.

(4) There is a good possibility that lasing can be achieved in the NO γ bands in NO-N_2-Ar mixtures. We are investigating this possibility by means of modeling studies and experiments. In this system, the NO(A) state is excited by transfer from the $N_2(A)$ state, which appears to have excellent energy storage properties.

REFERENCES

1. F. G. Houtermans, Helv. Phys. Acta 33, 933 (1960).

2. R. J. Carbone and M. M. Litvak, J. Appl. Phys. 39, 2413 (1968).

3. D. C. Lorents, R. M. Hill, and D. J. Eckstrom, "Molecular Metal Lasers," Semiannual Technical Report No. 1, Contract N00014-72-C-0478, Stanford Research Institute, Menlo Park, California (November 1972).

4. R. S. Mulliken, J. Chem. Phys. 52, 5170 (1970).

5. G. Herzberg, "Spectra of Diatomic Molecules," 2nd ed. van Nostrand, New York (1950). (expecially Chapter V and VI).

6. D. L. Huestis and W. A. Goddard III, Chem. Phys. Letters 16, 157 (1972).

7. S. L. Guberman and W. A. Goddard III, Chem. Phys. Letters 14, 460 (1972).

8. R. S. Mulliken, Phys. Rev. 136, A962 (1964).

9. T. E. Sharp, Atomic Data 2, 119 (1971).

10. S. L. Guberman, Thesis, California Institute of Technology, (1973). Available from University Microfilms.

11. E. U. Condon and G. H. Shortley, "The Theory of Atomic Spectra," Cambridge (1935).

12. W. Finkelnberg and Th. Peters, "Kontinuierliche Spectren," in Handbuch der Physik vol XXVIII, S. Flugge, ed., Springer-Verlag Berlin (1957).

13. R. Morgenstern, D. C. Lorents, J. R. Peterson, and R. E. Olson, "Differential Scattering of Metastable He(2^3S) on He(1^1S) at Energies Between 5 and 10 eV" Phys. Rev. A (in press).

14. H. A. Koehler, L. J. Ferderker, D. L. Redhead, and P. J. Ebert, App. Phys. 198 (1972); P. W. Hoff, J. C. Swingle and C. K. Rhodes, Optics Comm.(to be published); J. B. Gerardo and A. W. Johnson, IEEE Journal Quant. Elect. 9, 748 (1973).

15. P. W. Hoff, J. C. Swingle and C. K. Rhodes, App. Phys. Lett. 23, 245 (1973).

16. D. W. Setser, D. H. Stedman and J. A. Coxon, J. Chem. Phys. 53 1004 (1970).

17. R. A. Young and G. A. St. John, J. Chem. Phys. 48, 898 (1968).

18. D. C. Lorents and R. E. Olson, Semiannual Report No. 1, Contract N00014-72-C-0457, Stanford Research Institute (December 1972).

COLLISIONAL QUENCHING AND RADIATIVE DECAY OF THE MERCURY EXCIMER ‡

D. J. Eckstrom, R. M. Hill, D. C. Lorents, and H. H. Nakano

Stanford Research Institute
Menlo Park, California 94025

We have measured the molecular continuum radiation from Hg_2^* in the 4000-5000 Å range; the excitation was produced by a high energy, short pulse electron beam. When the excimer concentration is large, the dominant loss process is a bi-excimer collisional deactivation. At lower concentrations the decay becomes exponential and a radiative lifetime of the continuum radiation of 14 ± 3 μsec is measured.

Continuum radiation from molecular mercury has been the subject of investigation for more than 40 years,[1-8] but neither the spectroscopic assignments nor the radiative properties have been well established. Qualitatively, there are bands centered at 3350 and 4800 Å, which Mrozowski[2] and others have identified with transitions from the Hg_2^* (excimer) $^3\Pi_u$ and $^3O_u^-$ states to the repulsive $^1\Sigma_g^+$ ground state. There is also a band in the 5100-5700 Å range that may be distinct from the 4800 Å band.[8] In spite of interpretive uncertainties, the possibility of producing "dissociation" laser action in the 4800 Å band has been considered for some time,[9] with Carbone and Litvak[10] reporting a attempt to accomplish this in 1968.

‡ This research was supported by the Advanced Research Projects Agency of the Department of Defense and was monitored by ONR under Contract No. N00014-72-C-0478.

To determine some of the collisional and radiative properties of molecular mercury pertinent to analysis of its laser capabilities, we are studying the atomic and molecular radiation resulting from excitation of high-pressure Hg by an electron-beam pulse from a Febetron 706.[11] This device produces a 2 cm diameter, 3 nsec pulse of 500 kV electrons at an average current of approximately 7000 A. High-pressure mercury is produced in a heated stainless steel reservoir and cell fitted with brazed sapphire optical windows and an electron-beam window consisting of a stainless steel foil and a backup plate. Vapor pressures, measured directly with a mercury-filled bourdon gage connected by a capillary to the liquid mercury reservoir, are varied from 100 to 7600 torr. Temperatures of the cell and reservoir are monitored with thermocouples; the vapor pressures deduced from the reservoir temperatures agree with that measured directly within about 5%.

The measurements reported here consist of time-integrated photographic emission spectra and time-resolved emission spectra of selected molecular radiation. Microdensitometer traces of photographic spectra covering the 4000 to 5000 Å range at several pressures are presented in Figure 1. These traces show the blue molecular continuum band with superimposed atomic lines at 4047, 4078, and 4358 Å. The atomic radiation decreases in magnitude relative to the continuum with increasing pressure. This can be attributed to the collisional quenching of the states responsible for atomic radiation (Hg^{**}) by the process

$$Hg^{**} + Hg \rightarrow Hg^{*} + Hg, \qquad (1)$$

followed by excimer formation and radiation,

$$Hg^{*} + 2Hg \rightarrow Hg_2^{*} + Hg \qquad (2)$$

and

$$Hg_2^{*} \rightarrow 2Hg + h\upsilon. \qquad (3)$$

Processes (1) and (2) both become more rapid with increasing pressure. We have also found qualitatively that the intensities of the 3500 and 5400 Å bands decrease relative to that of the 4800 Å band as pressure is increased, consistent with earlier experiments.[4,6,7]

As seen in Figure 1, the blue continuum band was found to have a broad peak at 4570 Å. At low pressures, this band peak has been found to occur at 4850 Å.[4,5] This wavelength difference may result from a more complete vibrational relaxation of the excimers at the higher pressures of the present experiments.

A typical time-resolved intensity history of molecular radiation at 4570 Å is presented in Figure 2. We believe that the marked nonexponential behavior of this intensity history is due to the bi-excimer collisional deactivation of Hg_2^*:

$$Hg_2^* + Hg_2^* \xrightarrow{k} Hg_2^{**} + 2Hg. \qquad (4)$$

The rate equation, including this process and also spontaneous emission, is

$$\frac{dN}{dt} = -k(N)^2 - AN, \qquad (5)$$

where N is the concentration of Hg_2^* and A is the spontaneous emission coefficient. This equation has the solution

$$\frac{N_o}{N} = \left(\frac{kN_o}{A} + 1\right)e^{At} - \frac{kN_o}{A} \qquad (6a)$$

$$\tilde{=} 1 + (kN_o + A)\,t + (kN_o + A)(At^2/2). \qquad (6b)$$

The approximate form of the solution indicates that a graph of 1/N, or equivalently, of 1/intensity (since I = const · N), versus time will consist of linear and quadratic components that are associated predominantly with the bi-excimer collisional deactivation and with the spontaneous radiative decay, respectively. The data of Figure 2 are

presented in Figure 3 in the form 1/I versus t, where the linear component, dominant at early times, is clearly demonstrated.

Least squares curve fits of the exact equation (6a) to several intensity histories of the type presented in Figures 2 and 3 have allowed us to determine the parameters A and kN_0. We find that the radiative lifetime (1/A) of the continuum of Hg_2^* near 4570 Å is 14 ± 3 μsec independent of pressure over the range from 0.1 to 10 atm. For the data of Figures 2 and 3, we also find that $kN_0 \simeq 10^6$/sec. We have not yet measured N_0 independently, but estimates of its magnitude indicate that k is of the order of 10^{-11} cm^3/sec. The excellent fit of the curve representing equation (6a) to the data of Figure 2 gives confidence to the interpretation and to the parameters derived from the data.

In addition to the high spectral resolution measurements at 4570 Å, we have made time decay measurements on all three continuum bands, using filters that pass 3377 ± 10, 4880 ± 30, and 5145 ± 15 Å. These measurements were made at long times after the electron pulse ($25 \leq t \leq 75$ μsec) where the bi-excimer reaction (4) was no longer important. The photomultiplier tube was gated on after the beginning of the pulse to eliminate saturation effects and allow measurements of intensities several orders of magnitude below the peak values. These measurements indicate a common radiative lifetime of approximately 14 μsec for the entire continua independent of pressure, substantiating earlier observations of their common persistence.[1,4]

A purely exponential decay of all the bands with the same pressure independent time constant implies that the upper states for each band either are the same or are in collisional equilibrium throughout the decay, since in any other case the intensity decay would show pressure-dependent changes in the decay constants due to collisional transfer

effects. This would seem to rule out the interpretation assigning the 3500 and 4800 Å bands to $^3 1_u$ and $^3 0_u^-$ states with substantial energy differences, because in that case substantial collisional relaxation of the upper energy level would be expected.

REFERENCES

1. Lord Rayleigh, Proc. Roy.Soc. (London) A125, 1 (1929).
2. S. Mrozowski, Z. Physik 106, 458 (1937).
3. H. Takeyama, J. Science Hiroshima Univ. A15, 235 (1952).
4. A. O. McCoubrey, Phys. Rev. 93, 1249 (1954).
5. J. A. Berberet and K. C. Clark, Phys. Rev. 100, 506 (1955).
6. S. Penzes, H. E. Gunning, and O. P. Strausz, J. Chem. Phys. 47, 4869 (1967).
7. J. E. McAlduff, D. C. Drysdale, and D. J. LeRoy, Canada J. Chem. 46, 199 (1968).
8. M. Stupavsky, G.W.F. Drake, and L. Krause, Phys. Letters 39A, 349 (1972).
9. F. G. Houtermans, Helv. Phys. Acta 33, 933 (1960).
10. R. J. Carbone and M. M. Litvak, J. Appl. Phys. 39, 2413 (1968).
11. D. C. Lorents, R. M. Hill, and D. J. Eckstrom, "Molecular Metal Lasers," Semiannual Technical Report No. 1, Contract N000-14-72-C-0478, Stanford Research Institute, Menlo Park, California (November 1972).

FIGURE CAPTIONS

1. Microdensitometer Traces of Hg_2 Molecular Continuum Spectra. (Note shift of zero level for each curve).
2. Time History of Molecular Radiation at 4570 Å. (Pressure = 5270 torr.)
3. Inverse of Intensity Versus Time for Molecular Radiation at 4570 Å.

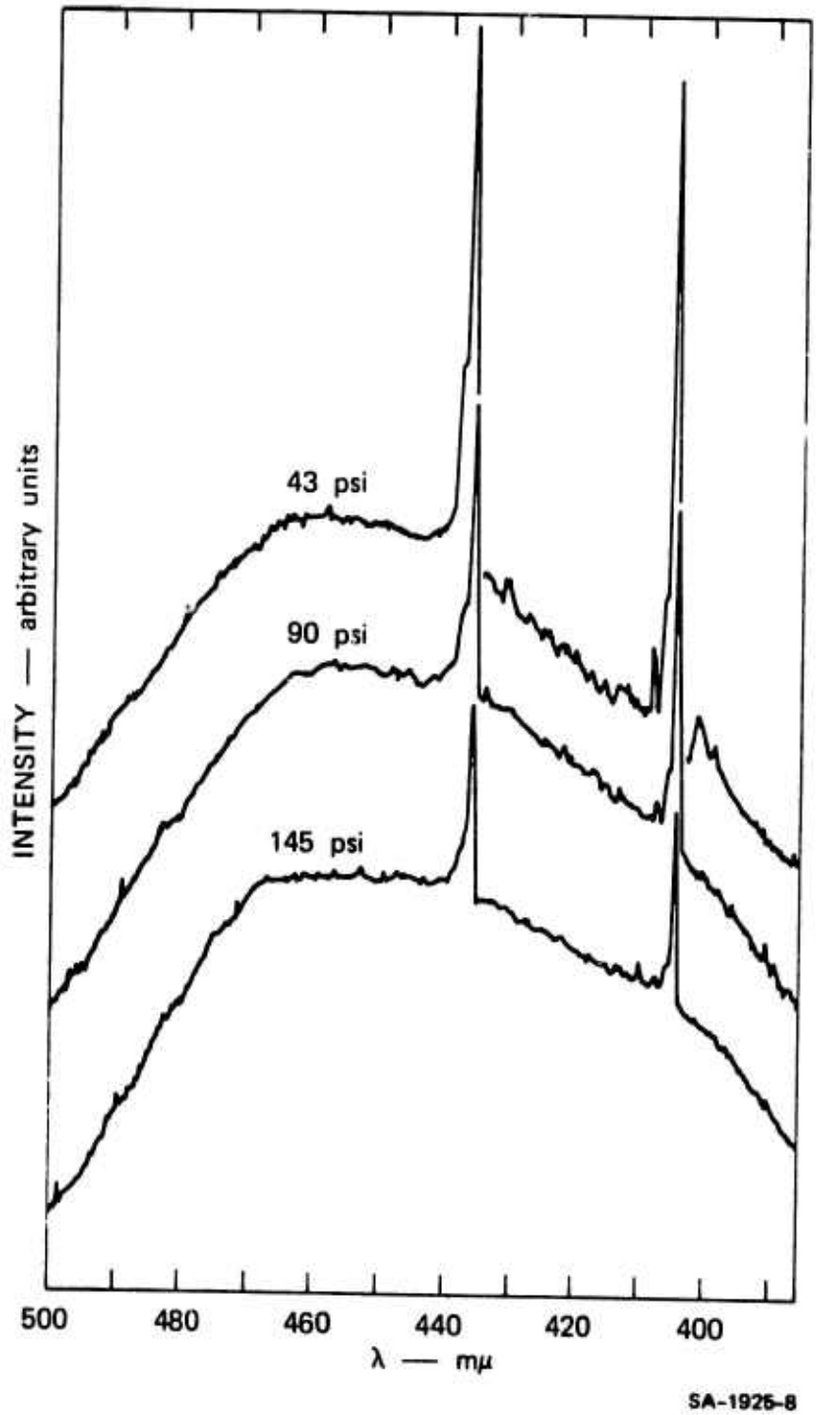
INTENSITY — arbitrary units
43 psi
90 psi
145 psi
500
480
460
440
420
400
λ — mμ
SA-1925-8

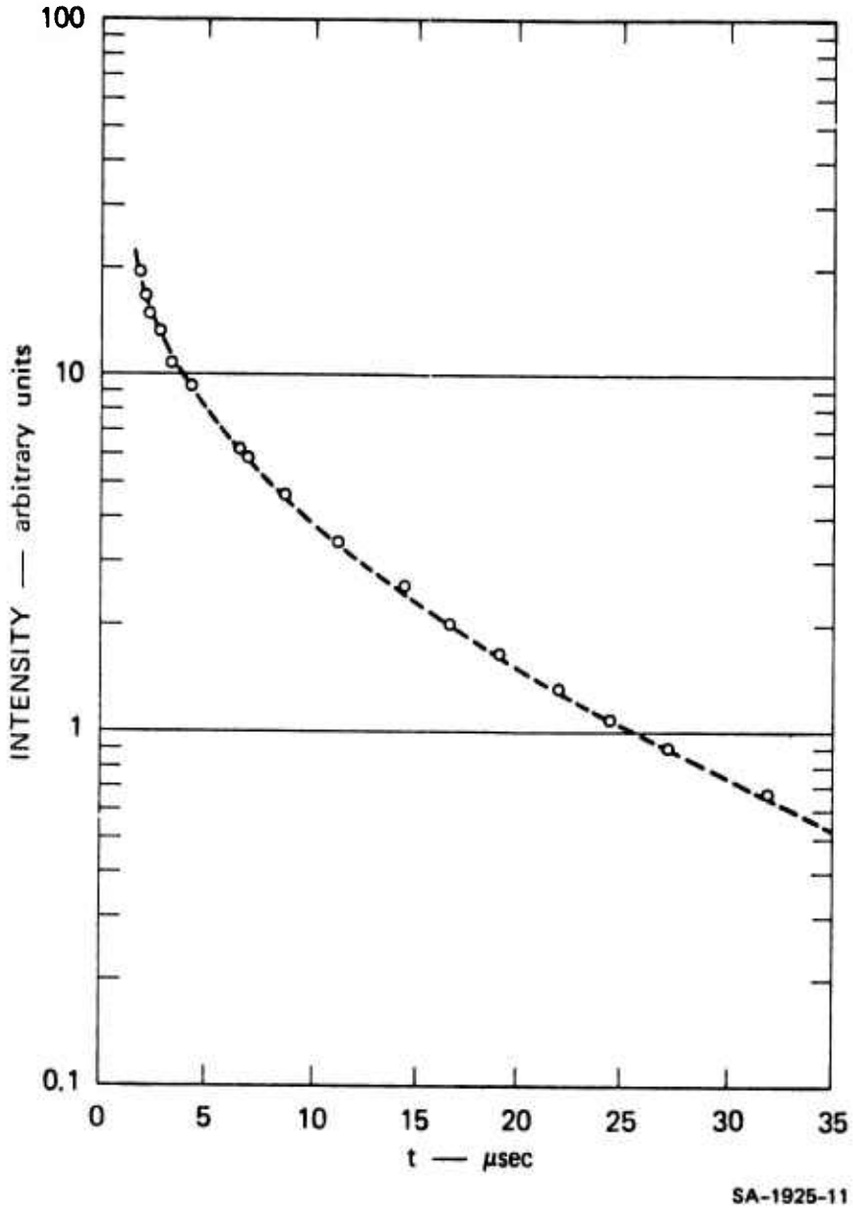
100
10
1
0.1
INTENSITY — arbitrary units
0
5
10
15
20
25
30
35
t — μsec
SA-1925-11

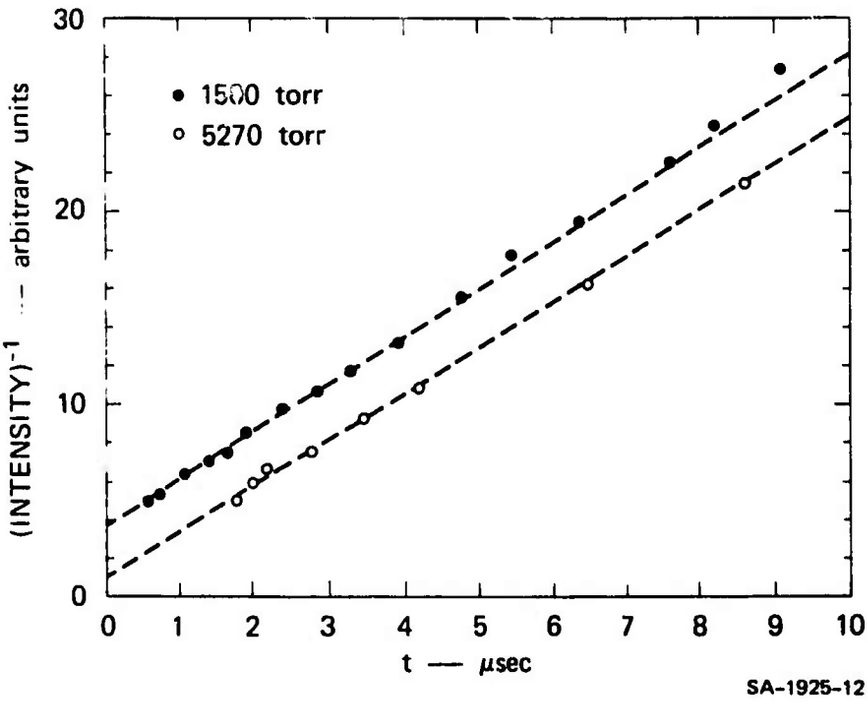
30
20
10
0
(INTENSITY)$^{-1}$ — arbitrary units
• 1500 torr
○ 5270 torr
0 1 2 3 4 5 6 7 8 9 10
t — μsec
SA-1925-12

MEASUREMENTS OF NEGATIVE GAIN FOR Hg_2 CONTINUUM RADIATION *

R. M. Hill, D. J. Eckstrom, D. C. Lorents, and H. H. Nakano

Stanford Research Institute
Menlo Park, California 94025

ABSTRACT

Gain measurements have been made at wavelength intervals over the continuum bands of high-pressure mercury excited by a short, high intensity electron beam pulse. These measurements, which utilized both continuum and laser light sources, showed net absorption at all wavelengths tested. This indicates that Hg_2^* has a larger cross section for absorption than for stimulated emission to the repulsive ground state, and virtually eliminates the chances of laser action on these transitions.

* This research was supported by the Advanced Research Projects Agency of the Department of Defense and was monitored by ONR under Contract No. N00014-72-C-0478.

SUBMITTED TO APPLIED PHYSICS LETTERS

Molecular mercury has been recognized for some time[1,2] as a possible medium for "dissociation" laser action similar to that currently being achieved in xenon and krypton[3]. This system radiates a broad continuum that has been divided, somewhat arbitrarily, into bands centered at 3500, 4800, and 5400 A.[4] The radiation is generally attributed to transitions from the stable excimer (Hg_2^*) states $^3\Pi_u$ and $^3O_u^-$ to the repulsive $^1\Sigma_g^+$ ground state. The excimer states are formed from the association of a metastable $Hg_2(^3P)$ atom with a ground state atom, $Hg(^1S_o)$, and stabilized in a second collision with a ground state atom. The repulsive ground state should ensure a population inversion on these continuum band transitions and lead to the prospect of tunable laser action, in particular, in the 4000-5000 A range.

We have been studying the kinetics of molecular formation and decay when Hg vapor at high pressures is excited by the 3 nsec, 500 keV, 7000 A electron pulse from a Febetron 706.[5] The vapor is contained in a heated stainless steel cell and reservoir of 2.5 cm i.d. by 25 cm length. Optical radiation is observed through sapphire windows, which are brazed to stainless steel flanges. The electron beam enters the cell perpendicularly to the optical path through a 1 mil Inconel foil. As part of this study, we recently reported a radiative lifetime of 14 ± 3 μsec for the continuum bands of Hg_2, measured at 3380, 4500, and 5400 A.[6] The lifetime was independent of pressure over the range from 1 to 10 atm.

In this note, we report the results of optical transmission measurements made between 3900 and 5145 A. The vapor pressure in these tests was approximately 2 atm; we estimate the excited gas optical path length at this pressure to be approximately 8 cm. Because of the bright spontaneous emission from excited mercury, an intense source of probing radiation is required. We used seven lines from a cw Ar^+ laser (Table I)

and also the continuum radiation from a 10 nsec, 10^3 watt flashlamp (Optitron Model NK-1). The probing radiation, together with the spontaneous radiation, was dispersed by a monochromator and detected by a photomultiplier. When the laser source was used, the photomultiplier was gated on 1 μsec before the electron pulse was fired in order to avoid saturation by the CW laser. When the continuum flash source was used, the monochromator slits were set for maximum width giving a 16 A resolution, and measurements were made every 20 A to give 80% coverage. The flash was fired approximately 30 nsec after the electron pulse, which was near the time for peak population of Hg_2^* molecules.

The percent transmission was determined by comparing intensities for the flashlamp radiating through unexcited Hg_2 and the flashlamp radiating through Hg excited by the electron pulse. The contribution of the spontaneous emission of Hg_2^* was subtracted out.

We found attenuation of the optical radiation at all wavelengths studied, when the mercury pressure was above one atmosphere. This is most clearly demonstrated in Figure 1a, which shows the attenuation of the cw laser radiation at 4766 A following excitation of the gas. Figure 1b shows the spontaneous emission at the same wavelength from the Hg_2^* excimers when the gas is excited under the same conditions but no probing radiation is incident. We have plotted the emission and absorption curves normalized at one time, in Figure 1c. The congruence of the time behavior shown by this plot allows us to conclude that the same species, Hg_2^*, is responsible for the spontaneous emission and the attenuation (negative gain).

The wavelength dependence of the absorption, determined in the flashlamp tests, is shown in Figure 2. Much of the scatter in the flashlamp data is due to pulse-to-pulse variations of the flash lamp

intensity. The general lack of structure, except near the atomic lines, indicates that the upper level of the absorptive transition is a repulsive upper electronic state of Hg_2, so that gain is unlikely anywhere in the continuum bands. A radiative lifetime of 14 μsec corresponds to a stimulated emission cross section of about 8×10^{-20} cm^2. It is not unreasonable to expect an absorptive process, even to a repulsive state, to have a larger cross section.

These results seem to rule out direct laser action on the Hg_2^* continuum. However, because of the relatively long radiative lifetime and small collisional losses,[6] Hg_2^* is still an attractive candidate for energy storage. It may be possible to utilize this energy storage property through an energy transfer mechanism to another radiative species. However the structure of the excited states of Hg_2 remains poorly understood. A practical use of Hg_2^* as an energy reservoir will require a better knowledge of its properties.

REFERENCES

1. F. G. Houtermans, Helv. Phys. Acta 33, 933 (1960).
2. R. J. Carbone and M. M. Litvak, J. Appl. Phys. 39, 2413 (1968).
3. H. A. Koehler, L. J. Ferderber, D. L. Redhead, and P. J. Ebert, App. Phys. 21, 198 (1972); P. W. Hoff, J. C. Swingle, and D.C.K. Rhodes, Optics Comm., to be published, App. Phys. Lett. to be published; J. B. Gerardo and A. W. Johnson, IEEE Jour. Quantum Elect., to be published.
4. W. Finkelnburg and T. Peters, Handbook der Physik XXVIII, Spectroskopie II (Springer-Verlag, Berlin, 1957).
5. D. C. Lorents, R. M. Hill, and D. J. Eckstrom, "Molecular Metal Lasers," Semannual Technical Report No. 1, Contract N00014-72-6-0478, Stanford Research Institute, Menlo Park, California (November 1972).
6. D. J. Eckstrom, R. M. Hill, D. C. Lorents, and H. H. Nakano, submitted to Chemical Physics Letters.

TABLE 1

Peak Attenuation of Ar^+ Laser Radiation by Hg_2*

Wavelength (A)	4579	4727	4765	4880	4965	5017	5145
Absorption (%)	10	23	25	15	6	7	5

FIGURE CAPTIONS

1. Time dependence of attenuation and emission at 4765 A following excitation of Hg at 40 psi.

   a. Attenuation of 4765 Ar^+ line. Intensity increasing downwards. The slight ringing is caused by gating the photomultiplier. When no excitation pulse occurs, only a flat trace is observed as shown.

   b. Spontaneous emission produced by excitation pulse from Febetron 706. No laser light is present. Zero base line shown for calibration.

   c. Attenuation and spontaneous emission plotted on same scale. Solid line is attenuation measurement; squares are the spontaneous emission; curves are normalized at 3.5 μ sec.

2. Percent transmission as a function of wavelength measured 30 nsec after excitation pulse. The transmission curves in the vicinity of the atomic lines at 4047 and 4358 Å have been defined in detail by measurements not shown here.

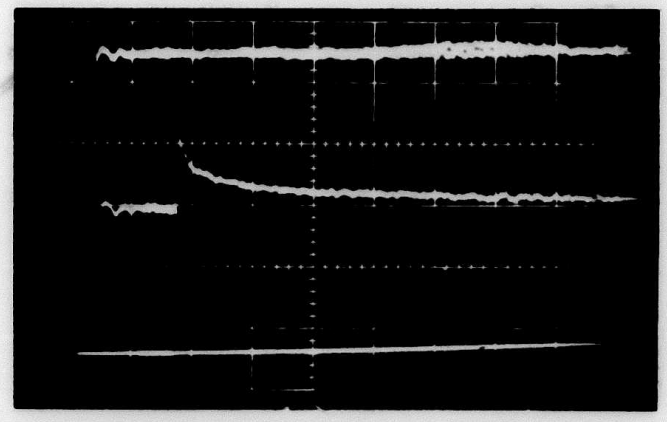

(a)

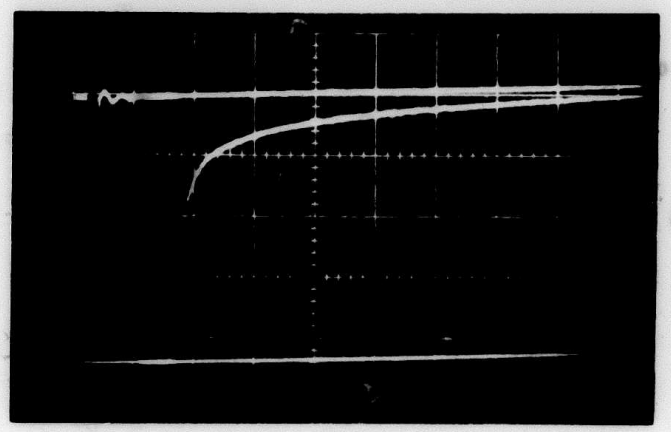

(b)

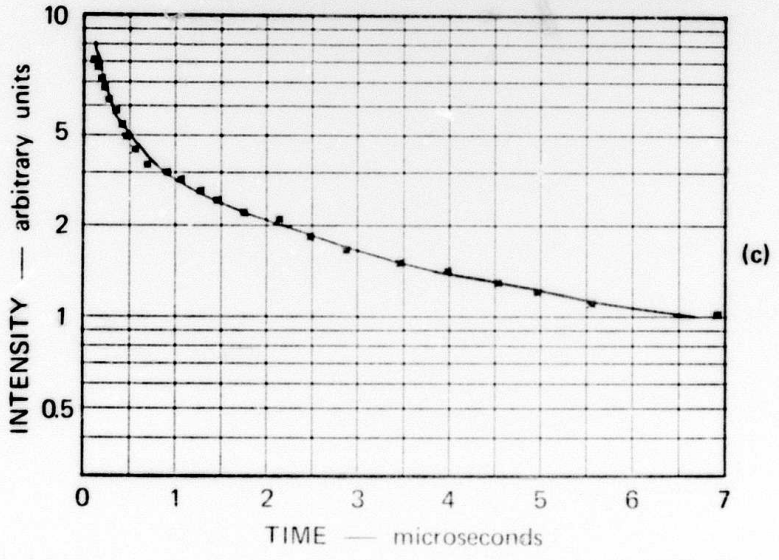

(c)

TA-1925-16

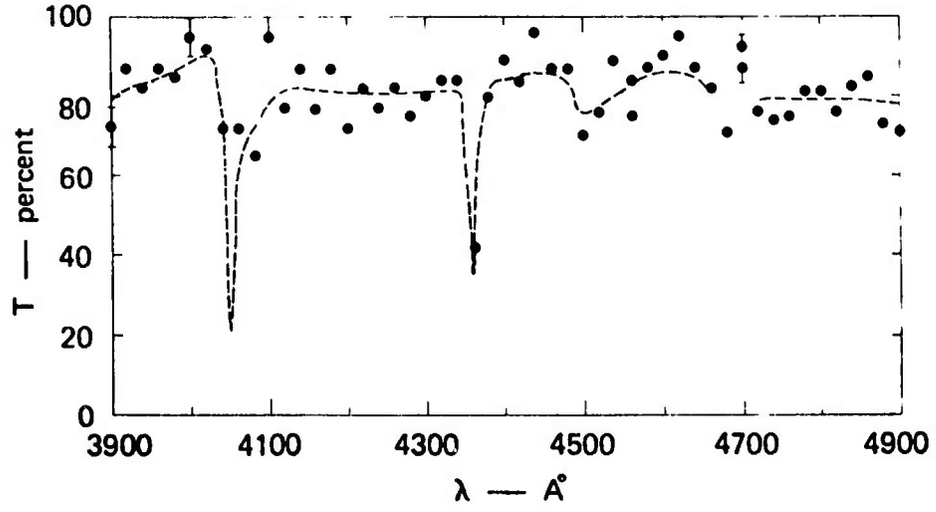

TA-1925-15